



RESEARCH ARTICLE

The liver kinase B1 supports mammary epithelial morphogenesis by inhibiting critical factors that mediate epithelial-mesenchymal transition

Kalliopi Tzavlaki¹ | Yae Ohata¹ | Anita Morén¹ | Yukihide Watanabe² |
Jens Eriksson¹ | Maiko Tsuchiya^{3,4} | Yuki Kubo⁵ | Kouhei Yamamoto⁵ |
Mikael E. Sellin¹ | Mitsuyasu Kato² | Laia Caja¹  | Carl-Henrik Heldin¹ |
Aristidis Moustakas¹ 

¹Science for Life Laboratory, Department of Medical Biochemistry and Microbiology, Biomedical Center, Uppsala University, Uppsala, Sweden

²Department of Experimental Pathology and Transborder Medical Research Center, Faculty of Medicine, University of Tsukuba, Tsukuba, Ibaraki, Japan

³Department of Oral Pathology, Graduate School of Medical and Dental Sciences, Tokyo Medical and Dental University, Tokyo, Japan

⁴Department of Pathology, Teikyo University School of Medicine, Tokyo, Japan

⁵Department of Comprehensive Pathology, Graduate School of Medical and Dental Sciences, Tokyo Medical and Dental University, Tokyo, Japan

Correspondence

Aristidis Moustakas.

Email: aris.moustakas@imbim.uu.se

Funding information

Magnus Bergvalls Stiftelse; Stiftelsen Lars Hiertas Minne; Vetenskapsrådet; Cancerfonden; H2020 European Research Council; OE och Edla Johanssons Stiftelse; Svenska Läkaresällskapetets Fonder; Ludwig Institute for Cancer Research; Barncancerfonden, Grant/Award Numbers: PR2020-0088, TJ2021-0078; Petrus och Augusta Hedlunds Stiftelse

Abstract

The liver kinase B1 (LKB1) controls cellular metabolism and cell polarity across species. We previously established a mechanism for negative regulation of transforming growth factor β (TGF β) signaling by LKB1. The impact of this mechanism in the context of epithelial polarity and morphogenesis remains unknown. After demonstrating that human mammary tissue expresses robust LKB1 protein levels, whereas invasive breast cancer exhibits significantly reduced LKB1 levels, we focused on mammary morphogenesis studies in three dimensional (3D) acinar organoids. CRISPR/Cas9-introduced loss-of-function mutations of *STK11* (*LKB1*) led to profound defects in the formation of 3D organoids, resulting in amorphous outgrowth and loss of rotation of young organoids embedded in matrigel. This defect was associated with an enhanced signaling by TGF β , including TGF β auto-induction and induction of transcription factors that mediate epithelial-mesenchymal transition (EMT). Protein marker analysis confirmed a more efficient EMT response to TGF β signaling in *LKB1* knockout cells. Accordingly, chemical inhibition of the TGF β type I receptor kinase largely restored the morphogenetic defect of *LKB1* knockout cells. Similarly, chemical inhibition of the bone morphogenetic protein pathway or the TANK-binding kinase 1, or genetic silencing of the EMT factor *SNAI1*, partially restored the *LKB1* knockout defect. Thus, LKB1 sustains mammary epithelial morphogenesis by limiting pathways that promote EMT. The observed downregulation of LKB1 expression in breast cancer is therefore predicted to associate with enhanced EMT induced by *SNAI1* and TGF β family members.

KEYWORDS

bone morphogenetic protein (BMP), epithelial-mesenchymal transition (EMT), liver kinase B1 (LKB1), morphogenesis, transforming growth factor β (TGF β)

This is an open access article under the terms of the Creative Commons Attribution-NonCommercial-NoDerivs License, which permits use and distribution in any medium, provided the original work is properly cited, the use is non-commercial and no modifications or adaptations are made.

© 2023 The Authors. *Journal of Cellular Physiology* published by Wiley Periodicals LLC.

1 | INTRODUCTION

The liver kinase B1 (LKB1 or serine/threonine kinase 11, STK11) is a central protein kinase that controls cell homeostasis and metabolism, since it regulates the activity of many kinases of the AMP-regulated protein kinase (AMPK) family, which in turn regulate the mammalian target of rapamycin kinases (Alessi et al., 2006). Active LKB1 kinase is assembled in a trimeric complex together with the adapter protein MO25 and the pseudokinase STRAD (Zeqiraj et al., 2009). Genetically, LKB1 is classified as a tumor suppressor protein because loss-of-function mutations in the kinase domain are seen in several human cancers or cancer-predisposing syndromes, such as lung and ovarian carcinomas and Peutz-Jeghers syndrome that predisposes carriers to hamartomatous polyp development in the intestine, followed by development of lung, intestinal and liver cancer (Alessi et al., 2006; Shackelford & Shaw, 2009). A tumor suppressive action of LKB1 causes cell cycle arrest in the early G1 phase via activation of p53 and its target gene, the cell cycle inhibitor p21^{WAF1/Cip1} (Tiainen et al., 2002). Loss-of-function *Lkb1* mutation in a mouse model of lung adenocarcinoma that expresses K-Ras pointed to the salt-inducible kinases (SIK), members of the AMPK family that become activated by LKB1, as mediators of the LKB1 tumor suppressor pathway (Hollstein et al., 2019; Murray et al., 2019).

Partitioning defective 4 (Par-4), the *Caenorhabditis elegans* LKB1 orthologue, regulates asymmetric division of early embryonic cells, causing differential fate to each daughter cell, that define embryonic polarity (Watts et al., 2000). In a conserved manner, *par-4/lkb1* regulates anterior-posterior embryonic polarity in *Drosophila melanogaster* (Martin & St Johnston, 2003). These developmental studies suggest that tumorigenesis caused by loss-of-function LKB1 mutations in humans might be linked to loss of cell polarity and control of asymmetric cell divisions in stem cells (Partanen et al., 2013). Inducible activation of LKB1 in single intestinal epithelial cells mobilize tight junctional and cytoskeletal assembly that support apical brush border formation (Baas et al., 2004). In dog kidney epithelial three dimensional (3D) cultures, proper epithelial morphogenesis requires coordination between peripheral actin contractility, centrosome orientation, and luminal membrane formation, based on the activity of LKB1 that signals to the small GTPase RhoA and downstream Rho kinase and myosin II pathway (Rodríguez-Fraticelli et al., 2012). In an equivalent system of lung epithelial luminal membrane differentiation, LKB1 can mediate its effect independent from its kinase activity and via direct association with the p114 RhoA guanine exchange factor (Xu et al., 2013).

An important cell system for the analysis of epithelial morphogenesis is the immortalized mammary epithelial cell model MCF10A, cultured under 3D conditions after embedding cells into an extracellular matrix (ECM) (Vidi et al., 2013). MCF10A 3D organoids have also been adapted to oncogenic signaling studies (Debnath et al., 2003). Upon LKB1 depletion, 3D MCF10A acini exhibited oncogenic hyper-proliferation, defects in cell polarity and abnormal protrusions of the acinar organoids, demonstrating a protective role of LKB1 during differentiation (J. Li et al., 2014; Partanen et al., 2007). Furthermore,

loss of *Lkb1* function in the mouse mammary gland causes abnormal branching morphogenesis of the mammary ducts (Partanen et al., 2012).

Epithelial-mesenchymal transition (EMT) is characterized by loss of E-cadherin and epithelial polarity, which promotes invasiveness and metastasis, and is potentially induced by transforming growth factor β (TGF β) signaling, via the TGF β type I and type II receptor kinases, SMAD (small and mothers against Dpp), ubiquitin ligases and protein kinases as signaling mediators (Lambert & Weinberg, 2021; Moustakas & Heldin, 2012; Tsubakihara & Moustakas, 2018). LKB1 overexpression in basal-type breast cancer cells suppresses EMT and partially restores E-cadherin expression (Rhodes et al., 2015). Alternatively, loss-of-function LKB1 has been associated with derepression of the EMT transcription factor SNAI1, which promotes cancer cell invasiveness (Goodwin et al., 2014). Accordingly, LKB1 negatively regulates TGF β signaling affecting various processes of cell differentiation and counteracting the potent action of TGF β as inducer of EMT, as previously demonstrated by us (Kahata, Dadrás, et al., 2018; Kahata, Maturi, et al., 2018; Morén et al., 2011). LKB1/AMPK signaling can also inhibit SMAD2 and SMAD3 phosphorylation by the TGF β type I receptor in breast cancer cells (N. S. Li et al., 2016; Lin et al., 2015). In ovarian cancer, LKB1 and its effector kinase SIK1 are deactivated, thus releasing TGF β signaling from negative regulation, promoting EMT and resistance to chemotherapeutic drugs (Hong et al., 2018).

All the above suggest that regulation of TGF β signaling by LKB1 is important in the context of normal mammary morphogenesis. We therefore generated MCF10A cells with a complete knockout of LKB1 using CRISPR/Cas9, and studied their acinar development in 3D organoid cultures. Our findings confirm and extend previous reports with milder (shRNA-based) LKB1 silencing in MCF10A cells (J. Li et al., 2014), and unequivocally show that signaling by TGF β family members and EMT transcription factors are major mediators of the abnormal developmental trajectory that 3D mammary organoids follow after LKB1 loss-of-function.

2 | MATERIALS AND METHODS

2.1 | Cell culture and treatments

MCF10A cells were cultured in Dullbecco's modified Eagle's medium (DMEM)/F12 (Invitrogen/Life Technologies/ThermoFisher Scientific), supplemented with 5% horse serum (HS) (Gibco, ThermoFisher Scientific), 2 mM L-glutamine, 100 U/ml penicillin and 100 μ g/ml streptomycin (Sigma-Aldrich AB), 20 ng/ml EGF (Pepro-Tech EC Ltd), 100 ng/ml cholera toxin (Sigma-Aldrich AB), 0.5 μ g/ml hydrocortisone (Sigma-Aldrich, AB), 10 μ g/ml insulin (Sigma-Aldrich, AB) (complete growth medium). Cells were starved in DMEM/F12 supplemented with 0.5% HS, 2 mM L-glutamine, 100 U/ml penicillin, 100 μ g/ml streptomycin, 100 ng/ml cholera toxin, 0.5 μ g/ml hydrocortisone, in the presence or absence of 10 μ g/ml insulin and 20 ng/ml EGF (starvation medium) for 16 h before treatment with

either 5 ng/ml TGF β 1 (PeproTech EC Ltd.) or 30 ng/ml BMP7 (a gift from K. Sampath, Sanofi-Genzyme Research Center). In the case of cotreatment with the TANK-binding kinase 1 (TBK1) inhibitor BX-795 (2 μ M; Millipore/Merck), the inhibitor was administered to the cells 30 min before TGF β stimulation. The AMP-analog 5-aminoimidazole-4-carboxamide-riboside (AICAR; Sigma-Aldrich; AB) was used at a 0.1 mM concentration for the time periods indicated in the figures.

For calcium depletion assays, cells were cultured in regular medium as described above, washed with phosphate buffered saline (PBS), incubated in PBS/5 mM EGTA (ethylene glycol-bis(β -aminoethyl ether)-N,N,N',N'-tetraacetic acid) at 37°C for 15 min and then cells were washed with PBS and cultured with the normal medium for various time points as indicated in the figures.

MCF10A acini were cultured in DMEM/F12, supplemented with 2% HS, 2 mM L-glutamine, 100 U/ml penicillin, 100 μ g/ml streptomycin, 100 ng/ml cholera toxin, 0.5 μ g/ml hydrocortisone, 10 μ g/ml insulin, 5 ng/ml EGF and 2% growth factor reduced matrigel (BD Biosciences) (assay medium). Eight-well chamber slides were coated with 40 μ l/well growth factor reduced matrigel, which was followed by a 15-min incubation in a cell culture incubator to allow matrigel to solidify. MCF10A parental or LKB1 knockout cells (5000 cells/well) were seeded on the bed of solidified Matrigel in assay medium as described above (seeding represents Day 0 of acinar morphogenesis). Cells were fed with fresh assay medium every 4 days (Days 4, 8, 12, and 16 of acinar morphogenesis).

Acinar cultures were treated with 5 ng/ml TGF β 1, 30 ng/ml BMP7, 2.5 μ M TGF β type I receptor kinase inhibitor LY2157299 (L2; Sigma-Aldrich; AB), 500 nM bone morphogenetic protein (BMP) type I receptor kinase inhibitor DMH1 (synthesized by the Ludwig Cancer Research Ltd.) and 2 μ M TBK1 kinase inhibitor BX-795 (Millipore/Merck). Dimethyl sulfoxide (DMSO, used at 1:1000–10,000 dilution) was the vehicle for the chemical inhibitors and 1 mM HCl, 0.1% bovine serum albumin (BSA) in PBS for the growth factors.

Acinar cultures were examined using a Zeiss Axiovert 40 CFL microscope and phase-contrast images were acquired using the \times 10 or \times 20 objective lens (Carl Zeiss; AB).

2.2 | Generation of *STK11* knockout MCF10A cells

STK11 knockout MCF10A cell clones were created using the CRISPR/Cas9 system. Four different single guide RNAs (sgRNAs) targeting the first exon of *STK11* gene were designed (Supporting Information: Figure S1a, Table S1). Forward and reverse oligonucleotides were annealed and extended to create 100 bp long dsDNA products using the Phusion High-Fidelity DNA polymerase (New England Biolabs; BioNordika; AB). DNA products were then purified using the polymerase chain reaction (PCR) purification kit (Qiagen AB), and inserted into the Afl II-cleaved/linearized gRNA_Cloning Vector (Addgene plasmid #41824) using the Gibson Assembly Master Mix (New England Biolabs, BioNordika, Sweden,

AB). MCF10A cells were transfected with the gRNA constructs along with the hCas9 expressing vector (Addgene plasmid #41815) using Eugene 6 (Promega; Biotech AB) according to the manufacturer's instructions. Transfected cells were selected with puromycin (Life Technologies/ThermoFisher Scientific) and were seeded at low densities in 10 cm plates (50, 100, and 250 cells/plate for each sgRNA). Single clones were picked up and expanded. Genomic DNA as well as protein lysate were isolated from each clone and successful knockout clones were confirmed by sequencing and immunoblotting.

2.3 | Genomic DNA isolation from MCF10A cells

MCF10A parental and potential LKB1 knockout cells were lysed in 500 μ l per sample lysis buffer (1% SDS, 50 mM Tris pH 8.0, 100 mM NaCl, 100 mM EDTA), supplemented with 0.5 mg/ml proteinase K, and were incubated at 60°C for 4–6 h. Lysates were then treated with 5 M NaCl (167 μ l/sample), followed by centrifugation at 13,200 rpm, for 10 min, at room temperature (RT). The supernatant was transferred into new tubes and was mixed with isopropanol at 1:1 ratio for the precipitation of DNA. Precipitated DNA was washed with 70% ethanol and was finally dissolved in TE buffer. PCR was performed to isolate and amplify DNA fragments surrounding the area targeted by the sgRNAs. The oligonucleotides used for PCR amplification were: forward, 5'-GAACACAAGGAAGGACCGCT-3', and reverse, 5'-CTGGCCTTGCTGAGTGAAA-3'. Sequencing of the amplified fragments was performed using the oligonucleotides 5'-ACAAGGAAGGACCGCTCAC-3' and 5'-GGAGAAGGAAGTCGGAACA-3' to verify mutations in *STK11*.

2.4 | Cell transfections with plasmids

Wild-type and kinase-dead (KD, engineered deletion of amino acids 192–195 in the kinase domain) human LKB1 expression vectors LKB1/pAHC and LKB1-KD/pAHC were kindly provided by Dr. Tomi P. Mäkelä (Tiainen et al., 2002). The respective LKB1 complementary DNAs (cDNAs) were epitope tagged with the hemagglutinin (HA) peptide in the N-terminal sequence of the LKB1 proteins. MCF10A parental and LKB1 knockout cells were transfected with plasmids using FuGENE 6 or FuGENE HD (Promega; Biotech AB) according to the manufacturer's instructions. For the generation of stable 22G-34 and 12L-15 + LKB1 rescue clones (22G-34R, 12L-15R) and stable 22G-34 + LKB1-KD rescue clone (22G-34R/KD), cells were transfected with LKB1/pAHC or LKB1-KD/pAHC and, 48 h after transfection, cells were cultured in the presence of 1 mg/ml geneticin (ThermoFisher Scientific) for 2 weeks. Then, individual overexpressing clones were selected and grown in culture medium, containing 0.5–1 mg/ml geneticin. The same protocol was used for transient transfections of the same cells with the LKB1 expression vectors followed by functional analysis at 48–96 h post-transfection.

2.5 | Immunoblotting

Total proteins were extracted from cells using lysis buffer containing 0.5% Triton X-100, 0.5% sodium deoxycholate, 20 mM Tris-HCl, pH 7.4, 150 mM NaCl, 10 mM EDTA supplemented with protease inhibitor cocktail (Roche Diagnostics Scandinavia AB) for 15 or 20 min on ice. The lysates were centrifuged at 13,000 rpm for 10 min at 4°C and the supernatant was transferred to new tubes. Protein concentration was determined using the bicinchoninic acid assay (Pierce/ThermoFisher Scientific). Equal amounts of protein samples were subjected to sodium dodecyl sulphate-polyacrylamide gel electrophoresis; resolved proteins were transferred on to PVDF (Millipore/Merck) or nitrocellulose (GE Healthcare Sweden) membranes, which were first blocked using 5% milk for 1 h at RT, and then incubated with the appropriate dilutions of primary antibodies overnight at 4°C. Membranes were incubated with horseradish-peroxidase secondary antibodies (Invitrogen/ThermoFisher Scientific, Stockholm, Sweden) diluted 1:10,000–20,000 and protein bands were visualized by enhanced chemiluminescence (ECL) using the Immobilon Western ECL reagent (Millipore/Merck). The primary antibodies used for immunoblot were: anti-LKB1 (sc-32245; Santa-Cruz Biotechnology), anti-STRAD α (sc-34102; Santa-Cruz Biotechnology), anti-MO25 (2027-1; Epitomics), anti-GAPDH (AM4300; Ambion, ThermoFisher), anti-p-AMPK α (Thr 172) (2535 S; Cell Signaling Technology), anti-AMPK (2532 S; Cell Signaling Technology), anti-p-SMAD2 (home-made), anti-SMAD2 (1736-1; Epitomics), anti-E-Cadherin (610182; Becton Dickinson Transduction Labs), anti-N-Cadherin (13116 S; Cell Signaling Technology), anti-ZO-1 (610966; Becton Dickinson Transduction Labs), anti-vimentin (5741 S; Cell Signaling Technology), anti-fibronectin (F3648; Sigma-Aldrich AB), anti-p-SMAD1/5/9 (9511 S; Cell Signaling Technology), anti-SMAD1 (ab33902; Abcam), anti-ID1 (sc-427; Santa-Cruz Biotechnology). The uncropped immunoblots used for all the representative figures presented here are listed in the Supporting Information.

2.6 | RNA isolation and gene expression analysis

Total RNA was extracted from cells using the Nucleospin RNA Plus kit (Macherey-Nagel GmbH & Co. KG) according to manufacturer's instructions. Each RNA sample was quantified using NanoDrop-2000 and equal amounts of RNA were reverse-transcribed using either the iScript cDNA synthesis kit (BioRad Laboratories AB) or the High Capacity cDNA Reverse Transcription kit (Applied Biosystems/ThermoFisher Scientific). Quantitative Real-Time PCR (qRT-PCR) was performed on a Bio-Rad CFX96 cycler (Bio-Rad Laboratories AB) using the qPCR-BIO SyGreen $\times 2$ Master Mix (PCR Biosystems). Gene expression levels of target genes were calculated using the $2^{-\Delta\Delta C_t}$ method and were normalized to the expression levels of GAPDH, HPRT1, or 18 s rRNA. A complete list of the oligonucleotides used is shown in Supporting Information: Table S2.

2.7 | Immunofluorescence (IF)

MCF10A parental and LKB1 knockout cells were fixed in 3.7% formaldehyde stabilized with 10% (v/v) methanol for 15 min at RT, followed by 2 washes, 5 min each, with PBS. The cells were then incubated in 0.1% glycine/PBS solution for 45 min at RT. Next, cells were permeabilized with 0.1% Triton-X-100/PBS for 10 min at RT and blocked with 5% BSA/PBS for 1 h at RT. After blocking, the samples were incubated with primary antibodies diluted in 1% BSA/PBS, overnight at 4°C. The next day, samples were washed twice with PBS and were then incubated with Alexa Fluor-546-labeled secondary antibody (Invitrogen; ThermoFisher Scientific) at a dilution of 1:500 in 1% BSA/PBS for 1 h at RT under darkness. F-actin staining was also performed using fluorescein-isothiocyanate labeled phalloidin, (1:1,000 dilution) (Sigma-Aldrich; AB) for 20 min at RT followed by 4',6-diamidino-2-phenylindole (DAPI) staining (1:1,000 dilution; Sigma-Aldrich, AB), for 5 min at RT. The samples were mounted in Fluoromount-G (SouthernBiotech; AH diagnostics) and examined using a Nikon Eclipse 90i microscope with a $\times 20$ objective. Images were acquired using the NIS-Elements Imaging Software. The primary antibodies that were used were: anti-E-cadherin (1:100; 24E10; Cell Signaling Technology; 3195 S) and anti-fibronectin (1:500; F3648; Sigma-Aldrich AB).

2.8 | IF of mammary epithelial acini

For the IF protocol, MCF10A parental and LKB1 knockout acini were grown in 8-well chambered glass bottom coverslips (Ibidi; GmbH) and were fixed in 2% paraformaldehyde for 20 min at RT. The cells were permeabilized with 0.5% Triton X-100/PBS solution for 10 min at 4°C and then washed 3 times with 0.1% glycine/PBS solution. Next, the samples were blocked with 5% FBS in IF wash buffer (PBS containing 7.7 mM Na $_3$, 0.1% BSA, 0.2% Triton X-100, 0.05% Tween-20) for 1 h at RT. The samples were then incubated with primary antibodies diluted in 5% FBS/IF wash buffer solution, overnight at 4°C. The next day, samples were allowed to heat up to RT to harden the matrigel and 3×20 min washes were performed with 0.1% glycine/PBS solution at RT. Then, they were incubated with Alexa Fluor-488-labeled secondary antibody (Invitrogen; ThermoFisher Scientific) diluted 1:200 in 5% FBS in IF wash buffer solution for 1 h at RT, followed a 20 min wash with IF wash buffer. The samples were rinsed twice with PBS and DAPI staining was performed (1 μ g/ml final concentration, for 20 min at RT). Samples were rinsed once more with PBS and finally each chamber was filled with 400 μ l PBS before examination with a Zeiss LSM700 confocal microscope with the Zeiss $\times 20$ objective lens (Carl Zeiss AB).

2.9 | Time-lapse imaging

Acinar structures were imaged in 8-well chamber slides (Falcon; ThermoFisher Scientific) on a custom-built microscope based on an

Eclipse Ti2 body (Nikon Minato), using a $\times 60/0.7$ Plan Apo Lambda air objective (Nikon) and a back-lit sCMOS camera with a pixel size of 11 μm (Prime 95B, Photometrics). The microscope chamber was maintained at 37°C in a moisturized 5% CO₂ atmosphere. Bright field images were acquired using differential interference contrast every 15 min for 70 h.

2.10 | Colony formation assay

For the colony formation assay, 3% low-melting point agarose (UltraPure™ Low Melting Point Agarose; Invitrogen; ThermoFisher Scientific) dissolved in H₂O, was diluted to 0.6% final concentration in MCF10A complete growth medium and was added into the wells of six-well plates (2 ml/well) to create the bottom layer. The six-well plate was incubated at 4°C for 1 h to solidify the agarose and then at 37°C for 30 min before adding the top cell-containing layer. For the top layer, 0.3% low-melting point agarose in MCF10A complete growth medium containing 2000 cells/ml was prepared and 1 ml of this cell-agarose mixture was added on top of the bottom layer of each well. Fresh feeder-layer (0.3% low-melting point agarose in MCF10A complete growth medium) was prepared and added on top (1 ml/well) weekly. After 21 days of incubation, the formation of colonies was examined using a Zeiss Axiovert 40 CFL microscope and phase-contrast images were acquired using the $\times 10$ objective lens (Carl Zeiss, AB). Moreover, colonies were stained with 0.1% crystal violet in 20% v/v methanol solution, by incubating for 1 h at RT, in darkness. The crystal violet solution was removed and seven washes with H₂O were performed to remove excess dye.

2.11 | ELISA

The concentration of secreted mature human TGF β 1 was measured in the conditioned medium of MCF10A parental and LKB1 knockout cells cultured in 2D and in the conditioned medium of MCF10A parental and LKB1 knockout acini grown in Matrigel, using human TGF β 1 Quantikine ELISA kit (R&D Systems Inc.) according to the manufacturer's instructions.

2.12 | Breast cancer patient samples

A total of 38 cases of primary breast cancer were analyzed. Tumors were selected from patients who had been surgically treated at the Tokyo Medical and Dental University Hospital. The tumors included ductal carcinoma in situ (DCIS) and invasive ductal carcinoma (IDC). Patients who had been treated before surgery were excluded. All the tumor samples were formalin-fixed and paraffin-embedded according to routine laboratory protocols.

All experimental procedures and use of clinical samples were approved by the ethics committee of the Faculty of Medicine, Tokyo Medical and Dental University (registration number M2000-1458).

All studies were conducted in accordance with the ethical guidelines of the amendment of the Declaration of Helsinki.

2.13 | Immunohistochemistry

Immunostaining for LKB1 was performed on formalin-fixed paraffin-embedded breast cancer tissue sections. Tissue slides were deparaffinized and incubated in 0.3% hydrogen peroxide solution for 30 min. Citrate buffer (pH 6.0) was used for heat-mediated antigen retrieval. Normal HS was used for blocking. Subsequently sections were incubated with the primary antibody (anti-LKB1 sc-32245) overnight at 4°C. The avidin-biotin complex method (Vector Laboratories) was used and coloration was achieved by the DAB detection kit (Vector Laboratories).

All of the slides were observed by two experienced pathologists (Y. K. and M. T.) Haematoxylin and eosin (H&E) staining was reviewed to ensure that the cancer tissue and adjacent nontumoral mammary epithelia were on the same section. An LKB1 score was calculated by multiplying the intensity score (negative = 0; weak = 1; moderate = 2; strong = 3) by the area score of stained cells (1%–24% = 1, 25%–49% = 2, 50%–74% = 3, 75%–100% = 4). The investigators were blinded to the patient information and other histopathological data. The final LKB1 score (ranging from 0 to 12) was determined after the two pathologists examined the slides independently and approved each score.

2.14 | Data analysis and statistics

Results express mean values of one up to three independent experiments (biological repeats) as explained in the figures. Error bars represent standard errors of the mean. Statistical analysis of the data was done using Excel or the Prism GraphPad v7.0 software. Two-group comparisons were performed using a two-tailed unpaired Student's *t*-test or the Mann–Whitney test as explained in the figure legends. When comparing the effects in different clones (MCF10A, LKB1 knockout, LKB1 knockout-rescued) the two-way analysis of variance (ANOVA) test followed by Tukey's multiple comparisons test was used (Figures 3, 6, 7, Supporting Information: S6, S8). When comparing more than two groups we used one-way ANOVA test followed by Dunnett's multiple comparisons test (Supporting Information: Figures S2, S3, S5, S6). Statistical significance is represented by *p* Values **p* < 0.05, ***p* < 0.01, ****p* < 0.001 or lack of significance by n.s. (not significant). Additional statistical methods are described in the previous method sections.

3 | RESULTS

3.1 | Invasive breast cancer exhibits low LKB1 expression

Before analyzing the function of LKB1 during mammary morphogenesis in 3D acini, we examined primary tissue from breast cancer

patients. Previous reports suggested that expression of E-cadherin, and estrogen and progesterone receptors, correlated with LKB1 expression in indolent tumors, whereas low LKB1 expression was observed in invasive and metastatic tumors of breast cancer patients (Chen et al., 2016; J. Li et al., 2014). Furthermore, women with higher LKB1 expression in their breast tumors exhibit better survival after endocrine therapy (Syed et al., 2019). In agreement with these earlier reports, the breast cancer patient cohort that we analyzed demonstrated strong epithelial and cytoplasmic staining for LKB1 in normal mammary tissue located adjacent to the resected tumors; the ductal epithelium was highly positive for LKB1 expression, whereas adjacent cell types, including myoepithelial cells were also positive (Figure 1a). Tumor tissue of intermediate aggressiveness, DCIS, exhibited weaker but clearly positive staining and in this case more cells with nuclear LKB1 signal relative to the normal tissue could be detected (Figure 1a,b). Finally, IDC tumors exhibited the weakest level of LKB1 expression in the tumor cells (Figure 1a). Quantification

of the immunohistochemical LKB1 signals confirmed the above observation and highlighted the gradual decrease of LKB1 expression from normal to more aggressive tumor tissue in the mammary gland (Figure 1b). These findings suggested that loss-of-function of LKB1 in normal mammary epithelial cells could generate abnormalities in tissue organization and contribute to tumorigenic transformation of the mammary epithelial cells.

3.2 | LKB1 knockout impairs acinar morphogenesis

We studied how LKB1 regulates mammary epithelial cell morphogenesis in 3D culture of MCF10A cells and after generating a complete LKB1 knockout using the CRISPR/Cas9 gene editing system, as described in the Supporting Information Results (Supporting Information: Figures S1-S3). We examined the efficiency of LKB1-depleted cells to form polarized acinar structures in 3D culture.

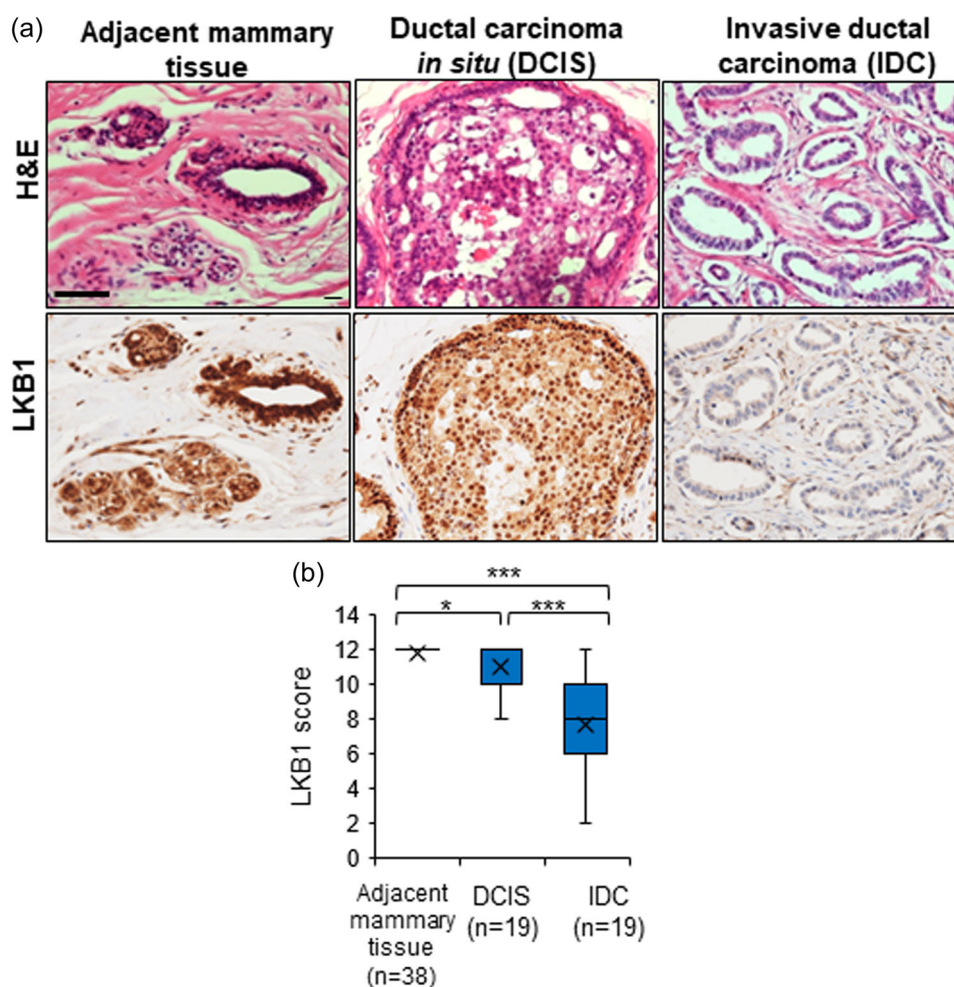


FIGURE 1 LKB1 expression in mammary carcinomas. (a) Immunohistochemical LKB1 staining of representative mammary carcinoma patient tissue, including adjacent “normal” mammary tissue, ductal carcinoma in situ (DCIS) and invasive ductal carcinoma (IDC). Haematoxylin and eosin (H&E) images are shown along with the LKB1-specific images. Scale bar, 20 µm. (b) Quantification of the LKB1 immunohistochemical signals in the indicated number (n) of patients as arbitrary LKB1 scores. The data are presented as box and whisker plots of the n replicates with median values (x) minimum and maximum values (whiskers), upper and lower quartile values (boxes), and p values shown based on a two-tailed unpaired Student's t-test. p Values *p < 0.05, ***p < 0.001. LKB1, liver kinase B1.

When cultured on a reconstituted basement membrane, MCF10A cells reorganize, start to proliferate and finally give rise to growth-arrested acinar organoids that consist of an outer polarized layer of epithelial cells and a hollow lumen in the center (Figure 2a), thus recapitulating features of the human mammary epithelium (Debnath et al., 2003). Already at day 5 during acinar morphogenesis, MCF10A parental cells had given rise to completely round structures, as expected, and 4 out of the 5 LKB1-depleted clones gave rise to organoids that exhibited loss of spherical organization, uneven morphology, abnormal cell growth, including generation of side-growths, as well as protrusions towards their microenvironment, all indicating loss of normal acinar morphogenesis (Figure 2b). Clone 17F-29 failed to form any kind of sphere-like or acinus-like structure in 3D conditions. At day 12 of acinar morphogenesis, parental MCF10A exhibited clear acinar features with a well-polarized translucent outer layer of epithelial cells surrounding a central hollow lumen after apoptosis of centrally located cells (Figure 2a,b). In contrast, *LKB1* knockout acini continued to present an uneven morphology, abnormal cell growth, and lacked hollow lumen (Figure 2b).

To gain more insight into the dynamic events taking place during acinar morphogenesis, we performed time-lapse imaging at different time periods of the morphogenetic program (Supporting Information: Movies S1–S6). At early stages of acinar morphogenesis (Days 4–6), parental acini developed by continuously rotating inside the surrounding basement membrane (Supporting Information: Movie S1). Notably, *LKB1* knockout organoids had completely lost this rotating capacity (Supporting Information: Movies S2, S3). At later stages of acinar morphogenesis (Days 9–12), rotational movement gradually decreased in parental acini as they matured and formed hollow lumen (Supporting Information: Movie S4). No lumen formation process was observed in *LKB1* knockout organoids while development of abnormal outgrowths and numerous protrusions invading the matrigel matrix were evident (Supporting Information: Movies S5, S6). Rotational motion during acinar morphogenesis has been previously reported in normal epithelial cell lines, but not in cancer cell lines, which are characterized by loss of polarity-related proteins, such as SCRIBBLE and PAR3, and aberrant microtubule organization (Wang et al., 2013).

E-cadherin immunostaining revealed well-formed cell-cell junctions between the cells of the outer polarized cell layer in the parental MCF10A acinar organoids, while in the *LKB1* knockout organoids, the staining was diffuse and only some cells exhibited well-developed adherens junctions (Figure 2c). Immunostaining of the acinar organoids for β -catenin revealed cytoplasmic localization in both MCF10A parental and *LKB1* knockout cells (Figure 2c), suggesting that activation of nuclear β -catenin may not be the cause of the abnormal 3D phenotype that *LKB1* knockout cells displayed. At the same time, the confocal microscopic analysis allowed us to verify the absence of hollow lumen in *LKB1* knockout organoids.

To confirm that the observed acinar phenotype (Figure 2b) was not an off-target effect, we stably overexpressed wild-type and KD *LKB1* in the knockout clone 22G-34 and wild-type *LKB1* in the

knockout clone 12I-15. *LKB1* expression was restored back to the normal MCF10A levels (Figure 2d, Supporting Information: Figure S4a; 22G-34R), which rescued to a large extent the formation of acinar organoids (Figure 2e, Supporting Information: Figure S4b). Attempted rescue using the KD *LKB1* mutant always resulted in lower expression levels of the mutant relative to the parental MCF10A level (Supporting Information: Figure S4a). The activity of the rescue *LKB1* constructs was monitored using phospho-AMPK immunoblot analysis (Supporting Information: Figure S4a); the very low (background) phospho-AMPK levels of the 22G-34 knockout cells remained the same in the KD *LKB1* clones (Supporting Information: Figure S4a). The organoids generated from the KD *LKB1* clones, always demonstrated a rough, moon-like morphology decorated by dense and peripheral protrusions or spikes of variable length, similar to the phenotype of the knockout cells, which nevertheless generated much longer protrusions (Supporting Information: Figure S4b). Thus, loss of *LKB1* induced a clear morphogenetic defect during mammary acinar organoid development.

3.3 | *LKB1* knockout activates TGF β auto-induction, early TGF β signaling, and TGF β -mediated EMT transcription factor expression

We have previously established that *LKB1* negatively regulates TGF β signaling (Morén et al., 2011). In the *LKB1* knockout organoids with defective acinar morphogenesis, ELISA for secreted mature TGF β 1 revealed enhanced TGF β 1 secretion when cells were cultured in 2D (Figures 3a) or 3D (Figure 3b). Accordingly, *TGFB1* messenger RNA (mRNA) expression was weakly enhanced in the absence of *LKB1* in 2D and 3D acinar cultures (Supporting Information: Figure S5a,b). Stimulation with exogenous TGF β for 2 h induced SMAD2 phosphorylation in both *LKB1* knockout and parental cells in a similar manner (Figure 3c). After 24 h of TGF β stimulation, SMAD2 phosphorylation was almost back to the basal levels in the parental cells, while in *LKB1* knockout cells p-SMAD2 levels were sustained (Figure 3c), indicating activation of prolonged TGF β signaling in the absence of *LKB1*.

One of the hallmarks of TGF β -induced EMT is the upregulation of EMT transcription factors, that is, *SNAI1*, *SNAI2*, *ZEB1*, and *ZEB2* (Kahata, Dadras, et al., 2018). Basal levels of expression of *SNAI1*, *SNAI2*, *ZEB1*, and *ZEB2* were enhanced by 1.5- to 4.0-fold when *LKB1* was depleted in 2D cultures (Supporting Information: Figure S5a); in 3D acinar cultures, it was mostly clone 22G-34 that exhibited 1.5- to 8.0-fold higher mRNA expression levels compared to the parental cells for the EMT transcription factors tested (Supporting Information: Figure S5b). This result is fully consistent with the profile of secreted mature TGF β 1 protein under 3D conditions (Figure 3b). Furthermore, upon stimulation with exogenous TGF β , *LKB1* knockout cells exhibited enhanced expression of TGF β -induced *SERPINE* and enhanced upregulation of *TGFB1* after 24 h (Figure 3d). *SNAI1* and *SNAI2* early upregulation by TGF β was stronger in *LKB1* knockout cells, and similarly, the induction of *ZEB1* and *ZEB2*, the two EMT transcription factors that are sequentially

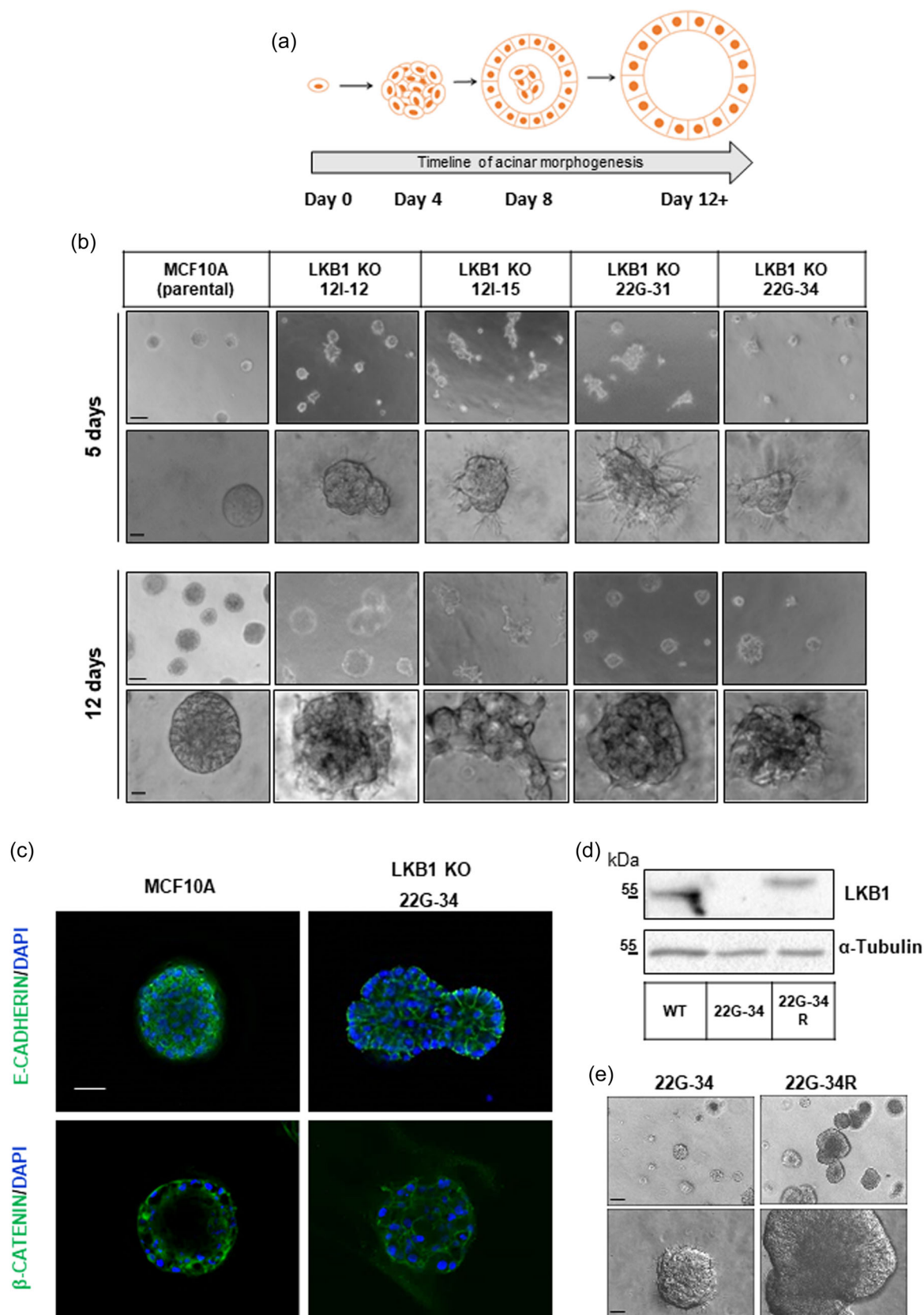


FIGURE 2 (See caption on next page)

induced by TGF β after *SNAI1*, was stronger in *LKB1* knockout compared to parental cells (Figure 3d). Basal expression levels of *TWIST1* and *TWIST2* were very low in MCF10A cells, and their expression was not affected by TGF β stimulation in wild-type or *LKB1* knockout cells (Figure 3d). These results thus suggest that *LKB1* expression inhibits TGF β auto-induction and TGF β -induced expression of EMT transcription factors (Figure 3e).

3.4 | Epidermal growth factor (EGF) and insulin support the EMT transcription factor profile of acinar development

MCF10A cells are cultured in the continuous presence of EGF and insulin, stimuli that contribute not only to the proliferation and survival, but also modulate the activity of TGF β signaling (Budi et al., 2015; Sundqvist et al., 2020). In the presence of EGF and insulin, the TGF β response was enhanced in *LKB1* knockout cells relative to parental cells (Supporting Information: Figure S6a), as demonstrated in the previous analysis (Figure 3d). In the absence of EGF and insulin, TGF β induced *SNAI1*, *SNAI2*, *ZEB1*, *ZEB2*, and *TGFB1* expression in both parental and *LKB1* knockout cells (Supporting Information: Figure S6b). However, the induction of these genes by TGF β was either unchanged or even attenuated in *LKB1* knockout cells (Supporting Information: Figure S6b). Examination of the basal expression levels of EMT transcription factor genes and *TGFB1* revealed that the enhanced basal expression levels in *LKB1* knockout cells grown in the presence of EGF and insulin (Supporting Information: Figure S6c), were decreased in the absence of these growth factors (Supporting Information: Figure S6d). Thus, EGF and insulin provide support to the basal expression of these genes, and the effect of *LKB1* probably depends on the signaling output of these growth factors.

3.5 | *LKB1* knockout cells bear an EMT phenotype

Next, we examined other hallmarks of EMT in the *LKB1* knockout cells grown in 2D, such as downregulation of E-cadherin and upregulation of mesenchymal fibronectin. Immunostaining experiments showed that E-cadherin decorated adherens junctions in parental cells, and phalloidin staining revealed cortical F-actin present at cell boundaries, as expected (Figure 4a). In *LKB1* knockout cells, E-cadherin, although

still expressed, was localized in the cytoplasm and the actin cytoskeleton was reorganized (Figure 4a), supporting the notion that *LKB1* knockout cells undergo EMT. In parental cells, TGF β treatment for 72 h did not significantly decrease E-cadherin expression, but its localization changed and mimicked to a certain extent the pattern observed in *LKB1* knockout cells (Figure 4a,b). In addition, remodeling of the actin cytoskeleton in parental cells in response to TGF β resembled the organization of actin in the *LKB1* knockout cells (Figure 4a). TGF β treatment delocalized even further E-cadherin and actin in *LKB1* knockout cells (Figure 4a), without decreasing the total levels of E-cadherin (Figure 4a,b). Moreover, *LKB1* knockout cells appeared flatter, were not as tightly packed as parental cells, and exhibited decreased ability to form cell-cell junctions, a phenotype that became even stronger in the presence of TGF β (Figure 4a).

We analyzed in more detail the assembly of adherens junctions by performing calcium depletion assays using EGTA treatment, which causes adherens junction disassembly and E-cadherin internalization. Following cell recovery, we monitored adherens junction reassembly using E-cadherin immunofluorescence microscopy (Supporting Information: Figure S7). Calcium depletion caused adherens junction disassembly in both parental and *LKB1* knockout cells (Supporting Information: Figure S7). However, parental cells built their new adherens junctions more efficiently than *LKB1* knockout cells, in which the reassembly was dispersed in few cells and polarization of the cell monolayer never was complete (Supporting Information: Figure S7). In contrast, the *LKB1* rescue cells also polarized faster and more quantitatively in these adherens junction reassembly assays (Supporting Information: Figure S7).

TGF β stimulation induced expression of fibronectin in parental cells and occasionally more so in *LKB1* knockout 22G-34 cells (Figure 4a). Immunoblot analysis revealed that fibronectin was strongly induced by TGF β in all cell models (Figure 4b). Levels of the tight-junction protein ZO-1 were roughly similar between parental and *LKB1* knockout cells (Figure 4b), and distinct formation of tight junctions was not evident, which agrees with a previous report (Fogg et al., 2005).

Examination of the *LKB1* rescue clones 22G-34R and 12I-15R confirmed the above findings. At the mRNA level, the well-established TGF β target genes and EMT factors, plasminogen activator inhibitor 1 (*PAI-1/SERPINE1*), *SNAI1*, *ZEB1* and *fibronectin* (*FN1*) demonstrated enhanced responses to TGF β stimulation in the 22G-34 *LKB1* knockout cells and this response decreased significantly upon *LKB1* re-expression (Supporting Information: Figure S8a). Immediate-early and direct TGF β responses such as phospho-SMAD2

FIGURE 2 Acinar morphogenetic potential of *LKB1* knockout MCF10A cells. (a) Diagrammatic representation of acinar morphogenesis by MCF10A cells. (b) Representative phase-contrast images of acini formed by parental MCF10A and *LKB1* knockout clones 12I-12, 12I-15, 22G-31, 22G-34, cultured in matrigel for up to 12 days. Images were taken at 5 and 12 days. Scale bars, 100 μ m (upper set of microphotographs); 20 μ m (lower set of photomicrographs). (c) Confocal microscopy immunofluorescence images displaying immunostaining of the proteins E-cadherin, β -catenin, and nuclear staining by DAPI in representative 14-day old acini formed by either parental MCF10A or *LKB1* knockout cells cultured in matrigel. Scale bar, 50 μ m. (d) Representative immunoblot of *LKB1* and α -tubulin (loading control) in parental MCF10A (WT), *LKB1* knockout 22G-34 and rescue 22G-34R cells. Molecular size markers in kDa are shown and original immunoblots are shown in Supporting Information: Figure S10. (e) Representative phase-contrast images of 12-day *LKB1* knockout 22G-34 and rescue 22G-34R acini cultured in matrigel. Scale bars, 100 (upper) and 20 (lower) μ m. *LKB1*, liver kinase B1.

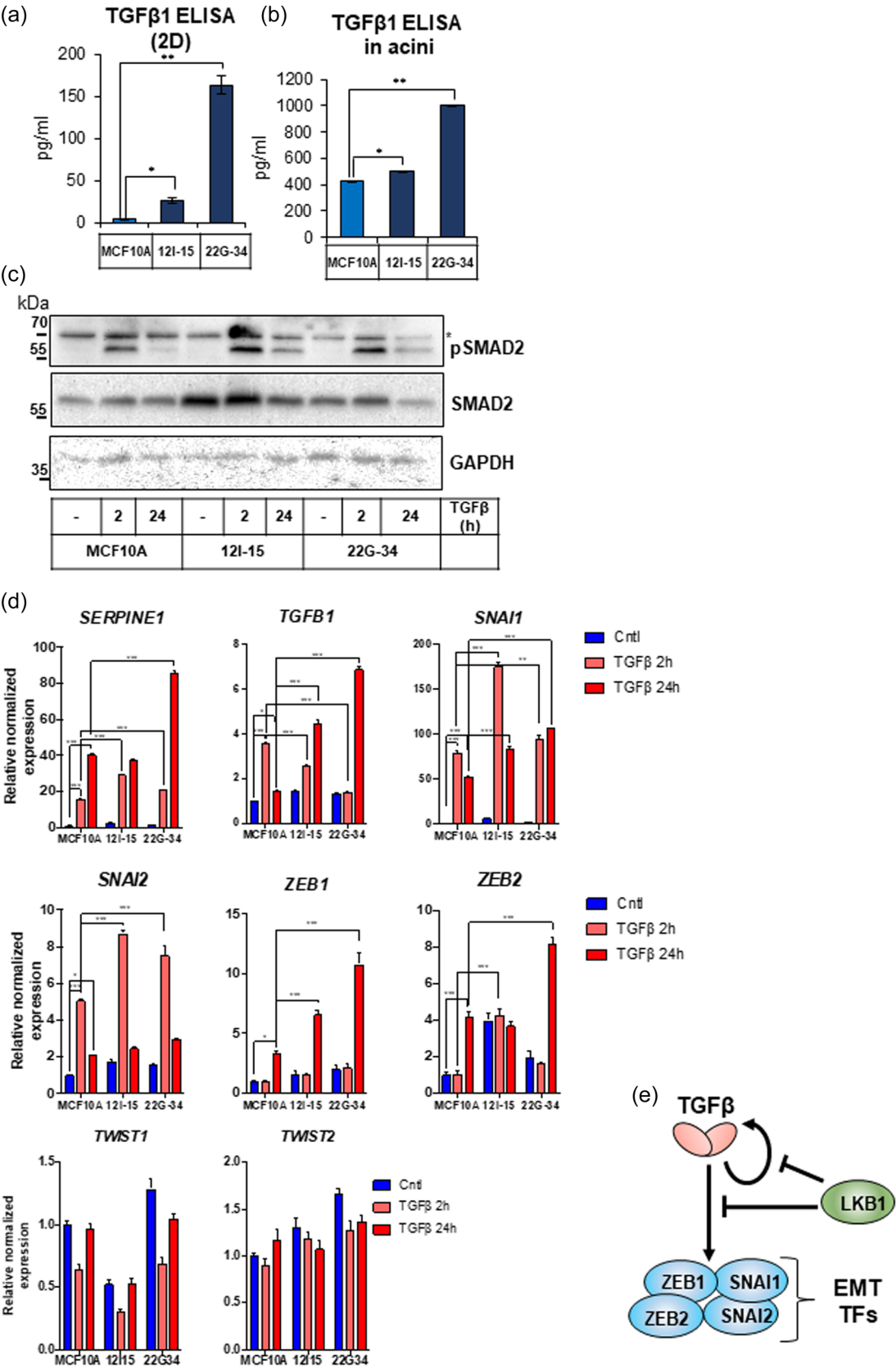


FIGURE 3 (See caption on next page)

levels, PAI-1 and SNAI1 protein induction were correspondingly enhanced in the knockout cells (22G-34 and 12I-15) and returned to reduced inducible levels in the rescue clones (note the nonsignificant change of phospho-SMAD2 levels between 12I-15 and 12I-15R rescue cells, presumably due to the lower levels of the re-expressed LKB1 protein relative to the equivalent re-expression in 22G-34R rescue cells; Supporting Information: Figure S8b-d). Among all target genes analyzed, the EMT/fibrogenic factors SNAI1 and fibronectin exhibited the most faithful response to the loss or re-expression of LKB1 under conditions of TGF β stimulation (Supporting Information: Figure S8b-d). When the kinase-defective LKB1 mutant was expressed, as described above (Supporting Information: Figure S4), the direct and immediate early TGF β responses of phospho-SMAD2 and SNAI1 protein remained unchanged relative to the knockout cells (Supporting Information: Figure S8e). However, the fibronectin and PAI-1 protein responses appeared weakly suppressed in the presence of the LKB1 KD mutant (Supporting Information: Figure S8e). These results should be interpreted with caution as we were unable to express the KD LKB1 mutant to the same level as wild-type LKB1, and especially, rescue of LKB1 knockout with the KD mutant in the 12I-15 cells was never successful (see the Section 4). All the above data, strengthened the notion that LKB1 knockout cells exhibit EMT and reduced polarization that could explain their defective acinar phenotype.

3.6 | A TGF β receptor kinase inhibitor normalizes the loss of acinar morphogenesis caused by LKB1 knockout

The enhanced early responsiveness of LKB1 knockout cells to TGF β stimulation suggested that inhibiting autocrine TGF β signaling in these cells might rescue the defect in acinar morphogenesis. We treated parental MCF10A cells with TGF β 1 and LKB1 knockout cells with LY2157299, a TGF β type I receptor kinase inhibitor (abbreviated L2), during acinar morphogenesis at different time points: at the onset of the experiment and every 4 days, up to day 12, when the experiment was terminated (Figure 5a). Exogenous TGF β decreased organoid size at Days 7 and 12, compared to the untreated organoids, a consequence of the reduced proliferation/growth arrest of

epithelial cells in response to TGF β (Figure 5a). The reduced proliferation observed was enough to prohibit the formation of a lumen by Day 12 during acinar morphogenesis (Figure 5a). In LKB1 knockout cells, L2 treatment did not result to any obvious morphogenetic effects by Day 7 (Figures 5a, 7 days). However, by Day 12, the acinar phenotype resembled the phenotype of parental organoids, with a hollow lumen in the center of the structure (Figure 5a, 12 days). Moreover, in the presence of the inhibitor, the abnormal outgrowth with the protrusions and the irregular shape were eliminated.

These experiments suggested that a critical time window for the sensitivity to L2 treatment could be the onset of cell polarization for the outer layer on one hand, and the cell death and lumen formation on the other (around days 6–8). Thus, we treated 3D cultures of parental and LKB1 knockout cells with TGF β and L2 inhibitor, respectively, on Day 8 (Figure 5b), and acinar morphogenesis was recorded prior (Day 7) and after (Day 12) treatment. By Day 7, normal acini had proliferated and grown in size, while the lumen started to form (Figure 5b, MCF10A, 7 days). After TGF β treatment, acini did not grow in size as much as the untreated cultures and spreading of cells outside the periphery of the acini was observed (Figure 5b, MCF10A, 12 days). Interestingly, initiating treatment of LKB1 knockout 3D cultures with the L2 inhibitor on Day 8 was sufficient to restore hollow lumen formation and normal acinar morphology (Figure 5b, LKB1 KO, 12 days), in a similar way as the repeated treatment with the inhibitor did (Figure 5a). Thus, enhanced auto-induction of TGF β signaling in LKB1 knockout cells is responsible for the defective acinar morphogenesis.

3.7 | The defective acinar morphogenesis in LKB1 knockout cells is partially rescued after inhibition of BMP signaling

We queried additional members of the TGF β family, for example, BMP, as contributors to abnormal acinar morphogenesis of LKB1 knockout acini. We first examined the responsiveness of MCF10A cells to BMP stimulation. BMP treatment induced phospho-SMAD1 levels in both parental and LKB1 knockout cells, induction that was slightly enhanced in LKB1 knockout cells, compared to parental cells

FIGURE 3 Enhanced TGF β secretion and increased levels of EMT transcription factors in LKB1 knockout mammary cells. (a, b) Concentration of secreted mature human TGF β 1, measured by ELISA, in the conditioned medium of parental MCF10A and LKB1 knockout cells cultured in 2D conditions (a), or as acini in matrigel for up to 12 days (b). The data are presented as mean values of triplicate determinations \pm SEM in bar graphs with *p* Values shown based on a two-tailed unpaired Student's *t*-test. (c) Representative immunoblot of p-SMAD2, SMAD2, and GAPDH (loading control) in parental MCF10A and LKB1 knockout cells that were either untreated or treated with 5 ng/ml TGF β for 2 or 24 h. Molecular size markers in kDa are shown and original immunoblots are shown in Supporting Information: Figure S10. A star in the p-SMAD2 immunoblot marks a background protein band. (d) qRT-PCR of *SERPINE1*, *TGFB1*, *SNAI1*, *SNAI2*, *ZEB1*, and *ZEB2* expression in parental MCF10A and LKB1 knockout cells in the absence (Cntl) or presence of 5 ng/ml TGF β stimulation for the time periods indicated. Representative data are presented as mean values of three technical replicates \pm SEM with *p* Values shown based on a two-way ANOVA test followed by Tukey's multiple comparisons test. (e) Schematic illustration of LKB1 attenuating TGF β auto-induction and TGF β -induced expression of EMT transcription factors (TFs). ANOVA, analysis of variance; LKB1, liver kinase B1; qRT-PCR, quantitative Real-Time polymerase chain reaction; SEM, standard errors of the mean; TGF β , transforming growth factor β .

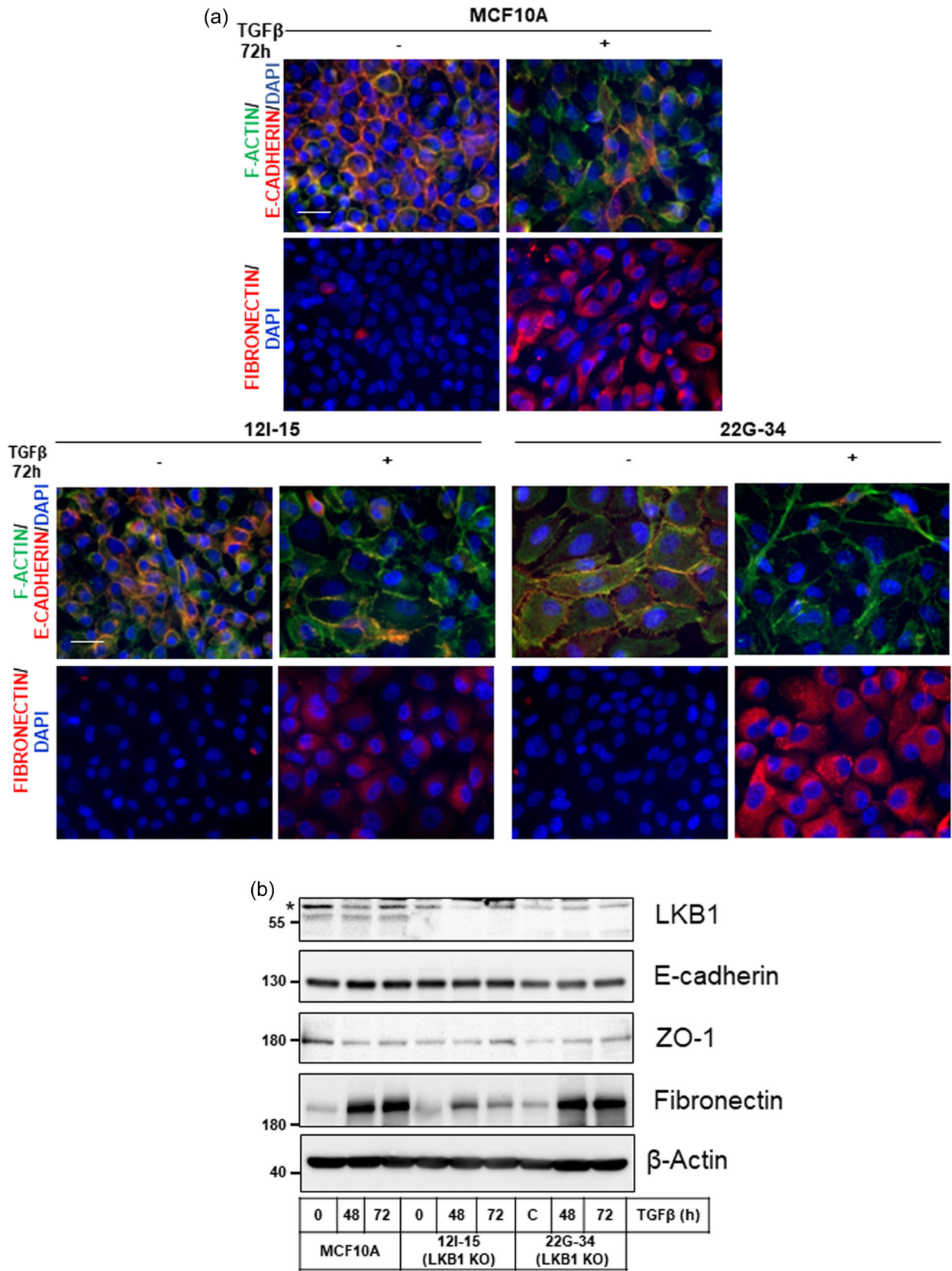


FIGURE 4 (See caption on next page)

at 2 h of stimulation (Figure 6a). BMP stimulation also induced similar levels of *ID1* expression in parental and *LKB1* knockout cells, while *SMAD7* induction was weaker in *LKB1* knockout cells (Figure 6b).

Following the same setup as before, we treated parental cells with BMP7 and *LKB1* knockout cells with DMH1, a BMP type I receptor kinase inhibitor (Figure 6c). By Day 7, BMP7 treatment resulted in perturbed normal morphogenesis of parental acini, as small outgrowths were observed, while by Day 12 the presence of the lumen was not as obvious as in the untreated acini and protrusions had emerged at the periphery of the BMP7-treated acini (Figure 6c). Conversely, DMH1 treatment slightly limited the abnormal aggregation of *LKB1* knockout outgrowths by Day 7, and restored to a large extent the abnormal acinar morphology by Day 12, yet the hollow lumen was not as well developed as in the parental cells (Figure 6c). When BMP7 was added on Day 8 in parental acinar cultures, a similar inhibitory effect on hollow lumen formation was recorded on Day 12 (Figure 6d). When DMH1 was added directly on Day 8 during acinus formation, a normalizing effect on *LKB1* knockout acini was achieved, similar to what was observed when repeated treatment of the inhibitor was performed (Figure 6d). Thus, inhibiting the kinase activity of the BMP type I receptors, phenocopies to some extent the TGF β inhibitor effect and suggests that both TGF β and BMP signaling are involved in the defective acinar morphogenesis caused by *LKB1* knockout.

3.8 | Inhibition of the TBK1 kinase partially rescues the defective acinar morphogenesis in *LKB1* knockout cells

Studies of breast cancer EMT have implicated the kinase TBK1 as a therapeutic target in ER α -positive breast cancer cells or as a mediator of platelet-induced EMT during breast cancer metastasis (Deng et al., 2014; Zhang et al., 2019). We therefore examined the impact of a specific TBK1 inhibitor (BX-795) on acinar morphogenesis. Parental and *LKB1* knockout acinar cultures were treated with BX-795 as indicated (Figure 7a). Parental acini developed normally in the presence or absence of TBK1 inhibitor and *LKB1* knockout acini continued to exhibit abnormal outgrowths and protrusions on Day 7, in the presence or absence of the TBK1 inhibitor (Figure 7a). However, by Day 12, significant normalization of the phenotype was observed, including the formation of a rudimentary hollow lumen, while enhanced peri-spherical protrusions were observed (Figure 7a). Extending the morphogenetic assay up to day 18, indicated that

TBK1 inhibitor treatment did not result in complete restoration of the phenotype in *LKB1* knockout 3D cultures (Figure 7a), as the TGF β inhibitor did (Figure 5). Whereas the hollow lumen had formed, acini continued to extend protrusions and cells extruded from the acini toward the matrix (Figure 7a). These results indicated that TBK1 is also implicated in the *LKB1* knockout phenotype, yet its contribution is distinct from that of TGF β and BMP signaling. Examining a possible crosstalk between TBK1 and TGF β signaling, we observed that the TBK1 inhibitor reduced the TGF β -induced expression of *SNAI1* and *SNAI2* in both parental and *LKB1* knockout cells, however, it had no significant effect on the TGF β -induced expression of *TGFB1*, *ZEB1* and *ZEB2* (Figure 7b). This selective effect of TBK1 on gene expression might reflect the difference in acinar phenotype restoration observed in Figure 7a, but further investigation is required to support this possibility.

3.9 | *SNAI1* is an important downstream mediator of TGF β signaling that controls abnormal acinar morphogenesis upon *LKB1* knockout

Since *LKB1* knockout cells exhibited clear signs of EMT and enhanced EMT responses to TGF β , including *SNAI1* expression (Figures 3, 4, Supporting Information: Figure S8), we addressed the role of *SNAI1* in abnormal acinar morphogenesis. Transient silencing of endogenous *SNAI1* reverted the enhanced *SNAI1* mRNA levels of *LKB1* knockout cells almost to the levels of the parental MCF10A cells when assayed at 24 and 48 h of TGF β stimulation (Figure 8a). *SNAI1* silencing was also evident at the protein level (Figure 8b; note the earlier time points of TGF β stimulation required to detect robust *SNAI1* protein levels in MCF10A cells). Notably, and as expected, silencing of *SNAI1* did not revert the TGF β -specific and direct signaling responses, including phospho-SMAD2, PAI-1 and fibronectin levels (Figure 8b). This analysis confirmed that silencing *SNAI1* did not act as a general inhibitor of TGF β signaling but rather affected the function of this specific EMT transcription factor.

Reduction of *SNAI1* expression yielded a clear acinar phenotype (Figure 8c). The abnormal acinar outgrowth, the enhanced protrusions into the matrix and the overall organization of the acini generated by *LKB1* knockout cells disappeared to a large extent (Figure 8c). Yet the acini did not undergo a fully normal development, since no clear lumen was evident in organoids where *SNAI1* was silenced (Figure 8c). We quantified the major phenotypic feature registered after *SNAI1* silencing, acinar protrusions to the matrix.

FIGURE 4 MCF10A *LKB1* knockout cells exhibit enhanced EMT response. (a) Representative immunofluorescence microscopy images for E-cadherin and fibronectin, and phalloidin staining for the visualization of F-actin, and nuclear DAPI costaining of parental MCF10A and *LKB1* knockout cells that were stimulated or not with 5 ng/ml TGF β for 72 h. Scale bar, 20 μ m. (b) Representative immunoblot of *LKB1*, E-cadherin, ZO-1 and fibronectin in parental MCF10A and *LKB1* knockout cells in the absence or presence of 5 ng/ml TGF β for the indicated time periods. β -Actin served as loading control. Molecular size markers in kDa are shown and original immunoblots are shown in Supporting Information: Figure S10. A star in the *LKB1* immunoblot marks a background protein band. EMT, epithelial-mesenchymal transition; *LKB1*, liver kinase B1; TGF β , transforming growth factor β .

Whereas 70% of *LKB1* knockout acinar organoids developed clear protrusions, only 20% of such organoids exhibited protrusions upon *SNAI1* silencing (Figure 8d). However, the impact of *SNAI1* silencing on the protrusion phenotype was not absolute, possibly reflecting incomplete silencing efficiency. The impact of TGF β stimulation on the extracellular protrusions to the matrix was not significantly

different (Figure 8d), whereas the major impact of TGF β , as we described earlier, was the significant reduction in organoid size (Figure 8e). Notably, although with a small effect, *SNAI1* silencing did interfere with the reduced size of organoids after TGF β stimulation (Figure 8e), suggesting that *SNAI1* may have a partial role in the antiproliferative function of TGF β . Thus, *SNAI1*, whose expression is enhanced once *LKB1* is lost, seems to control the invasive phenotype of the mammary acinar organoids.

4 | DISCUSSION

LKB1 is a tumor suppressor that regulates cell proliferation, polarity and central metabolism including protein synthesis, and loss of function mutations of *LKB1* are linked to the Peutz Jeghers syndrome and to an increased risk of developing cancer (Alessi et al., 2006; Shackelford & Shaw, 2009). The present study focuses on epithelial morphogenesis and demonstrates the importance of *LKB1* in maintaining homeostatic, physiological level of TGF β signaling during tissue patterning and growth. The most unexpected finding of this study was the difference in phenotype between exogenous TGF β stimulations on developing mammary acini, which led to reduced growth and size of the organoids, whereas enhanced autogenous TGF β signaling favored EMT and resulted in aberrant morphogenesis, instead of simply limiting organoid growth. This is an important new finding that extends our previous report regarding the role of *LKB1* as a negative regulator of TGF β signaling (Morén et al., 2011).

LKB1 forms a ternary complex with the adapter protein MO25 and the pseudokinase STRAD to achieve its functional kinase conformation (Zequiraj et al., 2009). *LKB1* knockout cells expressed similar or slightly lower levels of MO25 protein compared to parental cells, depending on the individual cell clone, while STRAD α protein expression was slightly decreased upon *LKB1* depletion (Supporting Information: Figure S3a). More detailed analysis of STRAD α and STRAD β mRNA expression indicated lack of changes in STRAD α

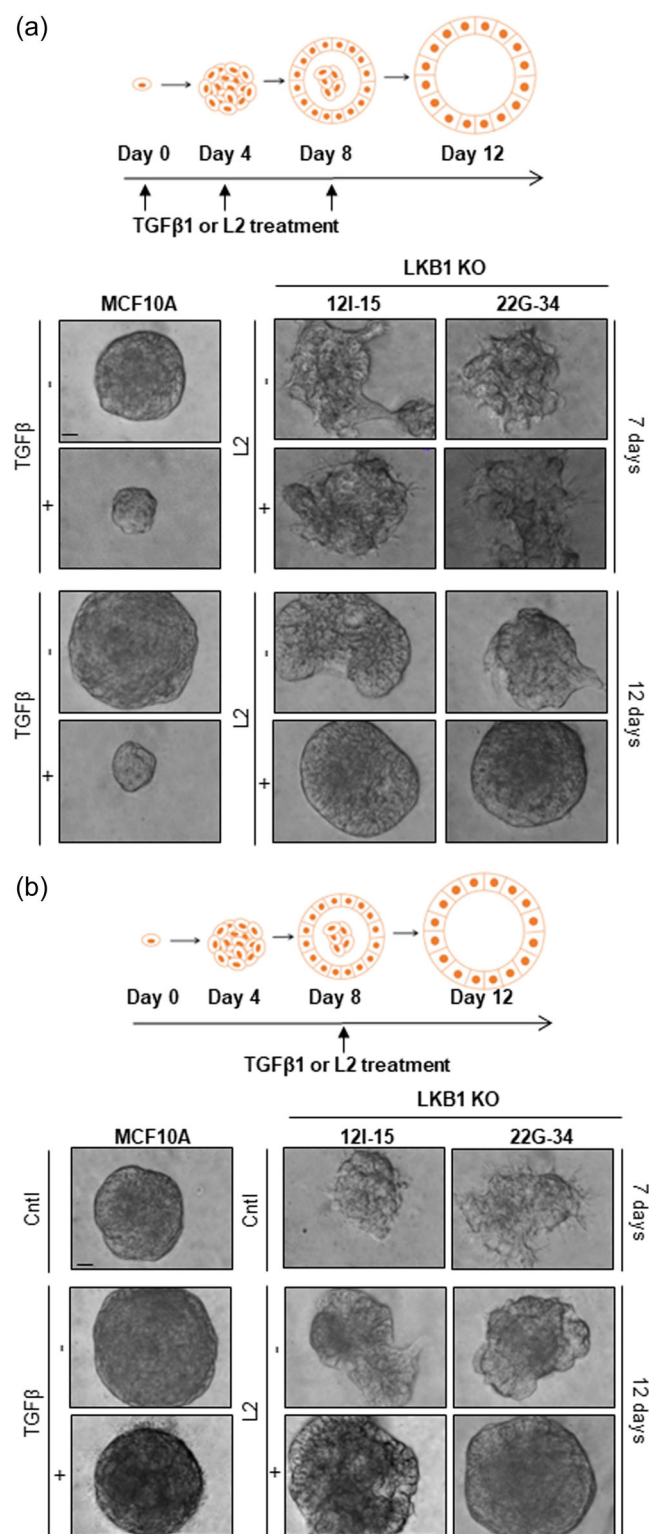


FIGURE 5 A TGF β type I receptor inhibitor rescues the defective acinar morphogenesis. (a) Top: schematic representation of the experimental design. Treatment started on Day 0 and was renewed when cultures were fed on Days 4 and 8 according to the scheme. Bottom: representative phase-contrast images of 7-day and 12-day parental MCF10A and *LKB1* knockout acini cultured in matrigel that were treated or not with either 5 ng/ml TGF β (in the case of parental MCF10A) or 2 μ M of the TGF β type I receptor kinase inhibitor LY2157299 (in the case of *LKB1* knockout cells). Scale bar, 20 μ m. (b) Top: Schematic representation of the experimental design. Treatment started on day 8 of acini development as described on the scheme. Bottom: representative phase-contrast images of 7-day and 12-day parental MCF10A and *LKB1* knockout acini that were treated or not with 5 ng/ml TGF β (in the case of parental MCF10A) or 2 μ M LY2157299 (in the case of *LKB1* knockout cells) for 4 days. Images were acquired before (7 days) and after the treatment (12 days). Scale bar, 20 μ m. *LKB1*, liver kinase B1; TGF β , transforming growth factor β .

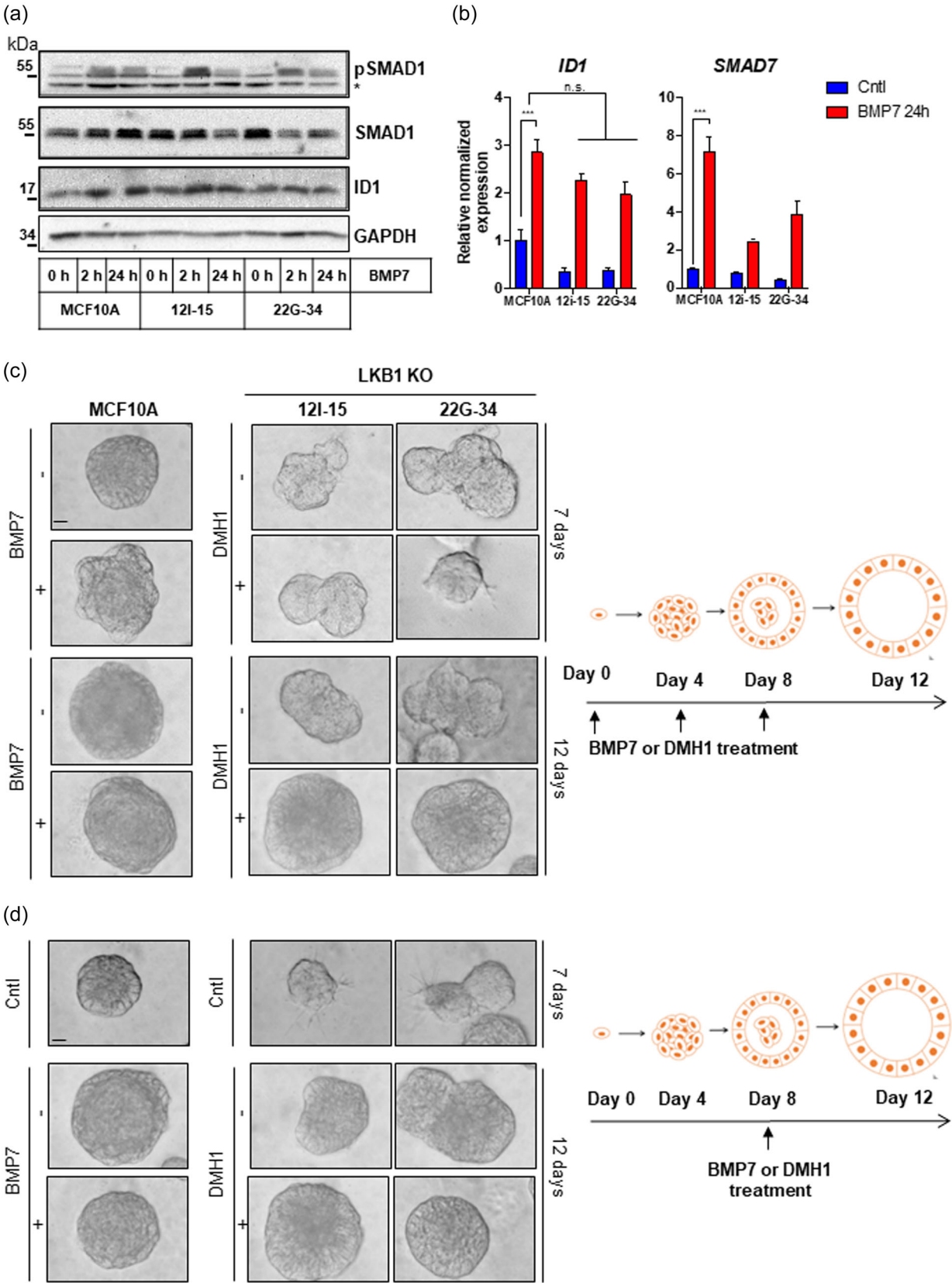


FIGURE 6 (See caption on next page)

mRNA and statistically significant increase of *STRADβ* mRNA by 1.15- to 1.87-fold (Supporting Information: Figure S3b). These data suggested possible adaptation of MO25 and *STRADα/β* to the loss of LKB1. However, no major loss or dramatic overexpression of the MO25/*STRAD* components was observed. In agreement with the established role of LKB1 as an upstream activator of AMPK family kinases (Shaw et al., 2004; Woods et al., 2003), *LKB1* knockout cells exhibited decreased levels of AMPK phosphorylation (Supporting Information: Figure S3d), which was rescued when cells were treated with the AMP analog AICAR (Supporting Information: Figure S3e). The latter is compatible with earlier reports demonstrating an LKB1-independent activation of AMPK phosphorylation by AICAR, a phenomenon that has been explained by the activation of AMPK (in the presence of AICAR) by additional compensatory protein kinases, such as ATM or calcium/calmodulin-dependent protein kinase kinase, under diverse cellular and physiological conditions (Jensen et al., 2007; Merlin et al., 2010; Sun et al., 2007). *LKB1* knockout cells showed a tendency to proliferate slower (Supporting Information: Figure S2a) even though LKB1 is known to cause growth arrest (Tiainen et al., 2002). Considering the 3D culture results and the role of TGFβ described in Figures 3, 5, and 8, enhanced TGFβ signaling could be responsible for the slower growth rate of these knockout cells. Yet, *LKB1* knockout cells had the capacity for anchorage-independent growth while parental cells did not (Supporting Information: Figure S2b), another finding supporting the tumor suppressing role of LKB1.

LKB1 depletion led to abnormal acinar morphogenesis, including abnormal overgrowth, loss of the spherical shape and extension of protrusions that invaded the surrounding matrigel (Figure 2). This phenotype agrees with a previous report on MCF10A cells oncogenically transformed by Myc or after shRNA-mediated LKB1 silencing (J. Li et al., 2014; Partanen et al., 2007). Moreover, the hollow lumen observed in parental acini was completely absent in the *LKB1* knockout organoids. Similar phenotypes, characterized by the absence of lumen and hyper-proliferation, have been reported in cases of depletion of polarity proteins, increased expression of antiapoptotic proteins, or when the expression of oncogenes is induced in MCF10A cells (Debnath et al., 2003; Muthuswamy et al., 2001; Reginato et al., 2005; Zhan et al., 2008). This phenotype was

successfully rescued to a large extent by restoring LKB1 expression, as lumen formation and lack of extended protrusions were recorded (Supporting Information: Figure 2d, e, s4b). Time-lapse imaging revealed that MCF10A parental acini rotate during the first days of acinar morphogenesis till the hollow lumen is formed, a point when they also become growth-arrested (Supporting Information: Movies S1, S4). *LKB1* knockout acini lost such rotational capacity, mimicking the phenotype generated after loss of the polarity proteins *SCRIBBLE* and *PAR3*, and showed dysregulated microtubule organization (Wang et al., 2013). Moreover, 3D acinar-like structures derived from cancer cell lines failed to undergo this rotational motion (Wang et al., 2013), supporting a role of LKB1 as a major upstream regulator of physiological cell polarity that couples to early acinus rotation. Immunostaining of β-catenin revealed clear cell-cell junctions among the outer polarized cells in parental acini; in *LKB1* knockout cells, β-catenin was still localized on the membrane even though acini had an abnormal phenotype with delocalized E-cadherin (Figure 2c). On the other hand, junctional E-cadherin staining was weak in either *LKB1* knockout or in parental acini. This suggests that delocalization of E-cadherin in *LKB1* knockout cells is not sufficient to induce a Wnt-like signaling pathway that mobilizes nuclear β-catenin.

The increased levels of secreted mature TGFβ1 in both 2D and 3D acinar cultures (Figure 3a,b), together with the enhanced and prolonged SMAD2 phosphorylation observed (Figure 3c), confirmed that LKB1 acts as negative regulator of TGFβ signaling in mammary organoids, as previously reported in studies of different cell types (Morén et al., 2011). The enhanced TGFβ auto-induction in *LKB1* knockout cells was linked to slightly enhanced basal expression levels of EMT transcription factors (Supporting Information: Figure S5), but these differences became even stronger after stimulation with TGFβ (Figure 3d). Removal of EGF and insulin from the MCF10A growth medium, had no significant impact on the induced expression of TGFβ-target genes of parental cells, but attenuated the enhanced TGFβ-induced and basal expression of EMT transcription factors and *TGFB1* in *LKB1* knockout cells (Supporting Information: Figure S6), suggesting a possible crosstalk of insulin or/and EGF signaling with LKB1. We therefore conclude that LKB1 signaling primarily affects regulation of direct TGFβ signaling target genes such as *SNAIL1*,

FIGURE 6 A BMP type I receptor inhibitor rescues the defective acinar morphogenesis. (a) Representative immunoblot of p-SMAD1, SMAD1, ID1, and GAPDH (loading control) in parental MCF10A and *LKB1* knockout cells after stimulation with 30 ng/ml BMP7 for the indicated time periods. Molecular size markers in kDa are shown and original immunoblots are shown in Supporting Information: Figure S10. (b) Representative qRT-PCR to determine *ID1* and *SMAD7* expression in parental MCF10A and *LKB1* knockout cells that were treated, or not (Cntl), with 30 ng/ml BMP7 for 24 h. Data are presented as mean values of three technical replicates ± SEM with *p* Values shown based on a two-way ANOVA test followed by Tukey's multiple comparisons test. (c) Right: Schematic representation of the experimental design. Treatment started on Day 0 and was renewed when cultures were fed on Days 4 and 8 according to the scheme. Left: representative phase-contrast images of 7-day and 12-day parental MCF10A and *LKB1* knockout acini cultured in matrigel, that were untreated or treated with either 30 ng/ml BMP7 (parental MCF10A) or 0.5 μM of the BMP type I receptor kinase inhibitor DMH1 (*LKB1* knockout cells). Scale bar, 20 μm. (d) Right: Schematic representation of the experimental design. Treatment started on Day 8 of acini development as described on the scheme. Left: representative phase-contrast images of 7- and 12-day parental MCF10A and *LKB1* knockout acini cultured in matrigel that were untreated or treated with either 30 ng/ml BMP7 (parental MCF10A) or 0.5 μM DMH1 (in the case of *LKB1* knockout cells) for 4 days. Scale bar, 20 μm. ANOVA, analysis of variance; BMP, bone morphogenetic protein; qRT-PCR, quantitative Real-Time polymerase chain reaction; LKB1, liver kinase B1; SEM, standard errors of the mean.

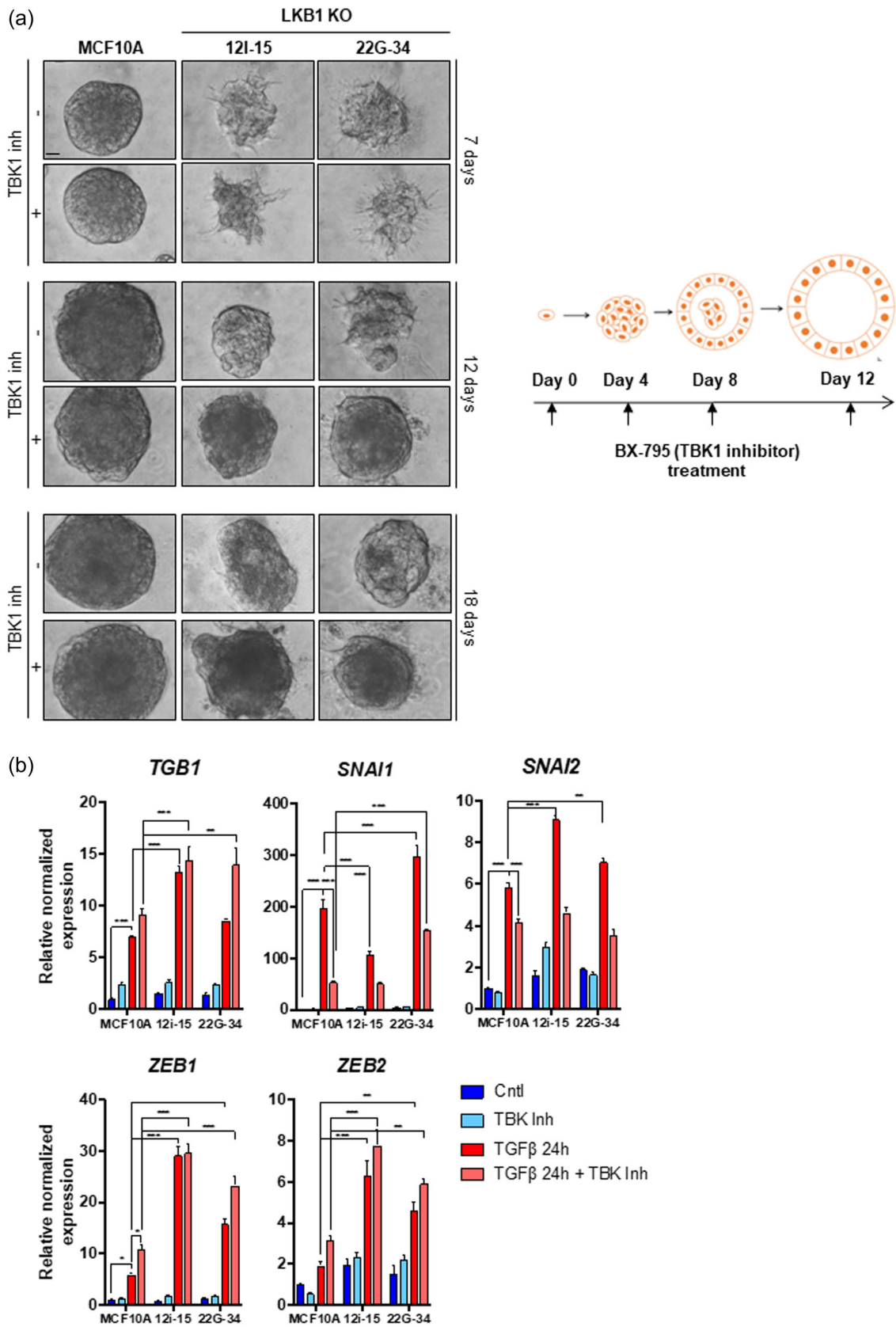


FIGURE 7 (See caption on next page)

among EMT transcription factors, and that EGF and insulin probably provide signals upstream of LKB1.

The enhanced EMT profile of *LKB1* knockout cells was further supported by immunostaining experiments where enhanced TGF β -inducible fibronectin was scored among different protein markers (Figure 4a). Fibronectin is downregulated during acinar morphogenesis, while exogenous fibronectin added in the surrounding matrix promotes overproliferation and increase in acinar size (Williams et al., 2008). Thus, enhanced TGF β signaling in *LKB1* knockout cells, in cooperation with increased fibronectin levels, provide the most plausible mechanism for the observed acinar overgrowth. E-cadherin expression levels were not as affected, but the localization of the protein was, suggesting that it is the targeting of E-cadherin to the cell membrane that is compromised in the *LKB1* knockout cells (Figure 4). This was confirmed by calcium depletion and adherens junction assembly experiments (Supporting Information: Figure S7). So far, the regulation of LKB1 localization by the presence of E-cadherin at the cell-cell junctions has been explored (Sebbagh et al., 2009), but a possible reverse mechanism has not yet been proposed.

Interrogating a requirement for active LKB1 protein kinase in cell-based or animal studies is not trivial as many reports provide conflicting evidence about a “true” kinase-inactive LKB1 mutant. Both cancer-derived LKB1 mutants and genetically engineered mutants have been employed in the literature, while rigorous studies of the kinase activity of such mutants is often missing (Fu et al., 2010; Marignani et al., 2001; Mehenni et al., 1998; Nezu et al., 1999; Shaw et al., 2004; Takeda et al., 2007; Tiainen et al., 2002). For this reason, we employed an engineered mutant causing a four amino acid (192–195) deletion in the LKB1 kinase domain that results in loss of kinase activity *in vitro* and in cells (Tiainen et al., 2002). Clones expressing the LKB1-KD mutant demonstrated persistence of peripheral protrusions and lack of a proper lumen during acinar development (Supporting Information: Figure S4b), while the response of these cells to TGF β was partially defective and partially rescued (Supporting Information: Figure S8e). Proper interpretation of these results requires deeper analysis and comparative studies of multiple mutants, as despite intense efforts, clones expressing KD LKB1 either failed or featured relatively low level of the mutant protein (Supporting Information: Figure S8e). These observations raise the interesting possibility that direct and immediate responses to TGF β signaling (phospho-SMAD2 and SNAIL) depend on the kinase activity of LKB1, as previously demonstrated (Morén et al., 2011), while more sustained responses (PAI-1, fibronectin) which also impact on the EMT and acinar morphogenesis independent from

TGF β , may depend on a scaffold-like, kinase-independent action of LKB1.

The defective acinar phenotype exhibited by *LKB1* knockout cells was rescued by treatment with LY2157299 (L2), a TGF β type I receptor kinase inhibitor (Figure 5), which suggests that the deregulated TGF β signaling and the EMT profile of *LKB1* knockout cells, is responsible for the development of abnormal acinar structures. Interestingly the effect of L2 treatment on acinar morphogenesis was observed from day 8 during acinar morphogenesis, around the time the lumen is starting to form and acini start to mature (Figure 5). Exogenous TGF β treatment could not perturb acinar morphogenesis similar to *LKB1* knockout. This must be so, since in normal MCF10A cells, oncogenic stimuli are missing that could generate necessary pro-oncogenic cooperation with TGF β signaling. For example, TGF β in cooperation with ErbB2, a member of the tyrosine kinase receptor family, give rise to acini with invasive protrusions (Seton-Rogers et al., 2004). TGF β induced growth arrest at the first stages during acinar morphogenesis and did not allow the growth and maturation of acini, while adding TGF β at later stages, led to acini of smaller size and to spreading of cells outside the periphery of acinar structures (Figure 5). These observations reflect the two opposing roles of TGF β , promoting growth arrest and enhancing EMT, cell migration and invasion. Silencing of SNAIL, a key downstream target of TGF β signaling in the EMT program (Tsubakihara & Moustakas, 2018), suppressed the *LKB1* knockout phenotype (Figure 8). SNAIL exhibited stronger action in the invasive, protrusion phenotype of the abnormal acini, as expected (Figure 8c,d). However, the weak effect observed on organoid size upon SNAIL silencing possibly suggests novel actions of SNAIL downstream of TGF β in the antiproliferative program. It is clear from this study that the impact of autogenous TGF β signaling that is homeostatically limited by LKB1 incorporates SNAIL and is not identical to acute stimulation of acini with exogenous TGF β . This differential effect is independent from oncogenic signaling, as the system that we analyzed is physiological and normal.

BMP signaling was not significantly affected upon LKB1 depletion, even though *LKB1* knockout cells did exhibit slightly higher SMAD1 phosphorylation compared to parental cells (Figure 6a,b). In mesenchymal lineage cell types, LKB1 strongly suppresses BMP signaling (Raja et al., 2016). However, treatment with the BMP type I receptor inhibitor DMH1 had a similar effect as the L2 inhibitor in restoring acinar formation in *LKB1* knockout cells even though lumen formation was not as efficient (Figure 6c,d). DMH1 is known to specifically inhibit the BMP type I receptors

FIGURE 7 A TBK1 inhibitor partially rescues the defective acinar morphogenesis of *LKB1* knockout cells. (a) Right: schematic representation of the experimental design. Treatment started at Day 0 and was renewed when cultures were fed on Days 4, 8, and 12 according to the scheme. Left: representative phase-contrast images of 7-, 12-, and 18-day parental MCF10A and *LKB1* knockout acini cultured in matrigel that were either untreated or treated with 2 μ M TBK1 kinase inhibitor BX-795. Scale bar, 20 μ m. (b) Representative qRT-PCR of *TGFB1*, *SNAIL1*, *SNAIL2*, *ZEB1*, and *ZEB2* expression in parental MCF10A and *LKB1* knockout cells treated with 2 μ M BX-795 or DMSO (control) and stimulated with 5 ng/ml TGF β for 24 h. Data are presented as mean values of three technical replicates \pm SEM with *p* Values shown based on a two-way ANOVA test followed by Tukey's multiple comparisons test. ANOVA, analysis of variance; LKB1, liver kinase B1; qRT-PCR, quantitative Real-Time polymerase chain reaction; SEM, standard errors of the mean; TGF β , transforming growth factor β .

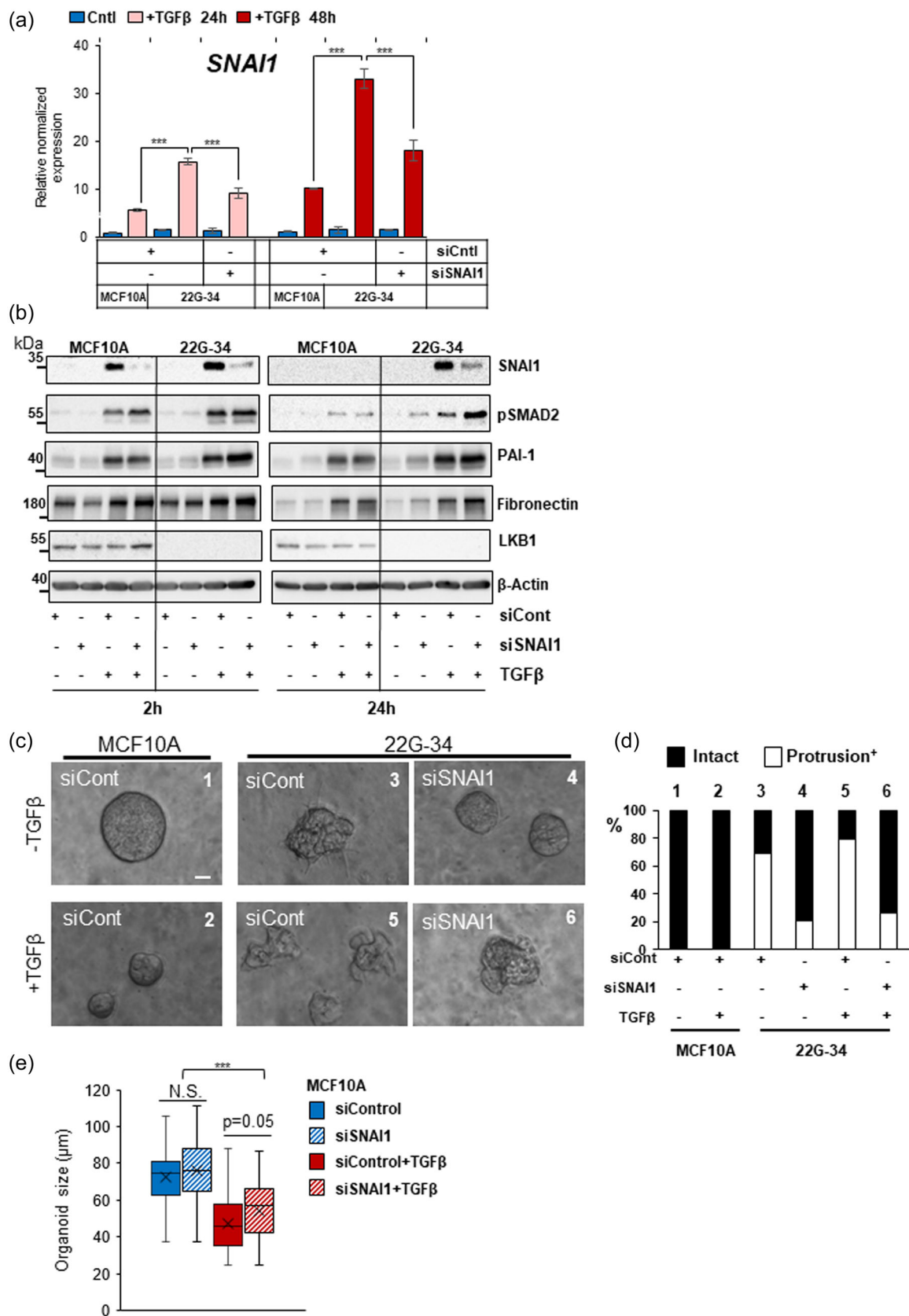


FIGURE 8 (See caption on next page)

known as activin receptor-like kinase 2 and 3 (ALK2 and 3) and thus block BMP-induced SMAD signaling (Hao et al., 2010), while the L2 inhibitor targets specifically the TGF β type I receptor ALK5 (Lahn et al., 2015). We therefore conclude that TGF β and BMP signaling are important for acinar morphogenesis and the results generated by the chemical inhibitors are not due to lack of specificity of these inhibitors. We anticipate that each pathway may offer distinct biological contributions to the abnormal acinar phenotype.

TBK1 kinase has been implicated in cancer progression via regulation of many biological processes, such as cell proliferation, survival and invasion (Cruz & Brekken, 2018), and it is involved in the platelet-induced EMT in breast cancer cells (Zhang et al., 2019). The effect of the TBK1 inhibitor BX-795, which also led to a partial rescue of the LKB1 knockout phenotype, was different compared to the effects of L2 or DMH1, as lumen formation was more pronounced, invasive protrusions did not disappear and relatively smaller acini appeared (Figure 7a). TBK1 may thus impact on acinar morphogenesis in distinct ways compared to TGF β signaling, affecting subsets of TGF β responses (e.g. *SNAI1*, *SNAI2*) (Figure 7b), and responses related to enhanced cell survival and antiapoptotic signals.

The relative loss of expression of LKB1 in aggressive breast tumors (Figure 1) proposes that such IDCs may exhibit strong TGF β , BMP, and TBK1 signaling, whereas they may also exhibit signs of EMT with important functional roles for *SNAI1*. Although the importance of TGF β and EMT in invasive breast carcinomas is established, the new evidence provided here suggests a model whereby the importance of LKB1 expression or loss thereof is worth considering in future studies of breast cancer development. Overall, our findings support that LKB1 plays a crucial role during epithelial cell differentiation and acinar formation, and its depletion leads to an abnormal phenotype that can be significantly attributed to deregulated TGF β -*SNAI1*/BMP and TBK1 signaling. Thus, normal mammary morphogenesis makes use of the physiological LKB1 pathway to limit the actions of TGF β family members and to protect the developing tissue from aberrant EMT signals.

AUTHOR CONTRIBUTIONS

Aristidis Moustakas conceived and Kalliopi Tzavlaki implemented after fundamental adaptations the project; Kalliopi Tzavlaki, Aristidis Moustakas, Yae Ohata, Yukihide Watanabe, and Mikael E. Sellin designed experiments; Kalliopi Tzavlaki, Anita Morén, Yae Ohata, Yukihide Watanabe, Jens Eriksson, Yuki Kubo, Maiko Tsuchiya, Kouhei Yamamoto acquired data; Kalliopi Tzavlaki, Aristidis Moustakas, Yukihide Watanabe, Jens Eriksson, Yae Ohata, Yuki Kubo, Maiko Tsuchiya, and Kouhei Yamamoto analyzed data; Kalliopi Tzavlaki, Laia Caja, Yukihide Watanabe, Mitsuyasu Kato, Jens Eriksson, Mikael E. Sellin, Carl-Henrik Heldin, Yae Ohata, Yuki Kubo, Maiko Tsuchiya, Kouhei Yamamoto and Aristidis Moustakas interpreted data; Aristidis Moustakas, Yae Ohata, Carl-Henrik Heldin, Mitsuyasu Kato, Laia Caja, Maiko Tsuchiya provided funds to the project; Aristidis Moustakas and Laia Caja supervised the project; Kalliopi Tzavlaki, Yae Ohata and Aristidis Moustakas managed the collaborative work; Kalliopi Tzavlaki wrote and Aristidis Moustakas revised the original manuscript; Anita Morén, Yae Ohata performed all experiments during the revision; Aristidis Moustakas, Kalliopi Tzavlaki, Yae Ohata, Mikael E. Sellin, Carl-Henrik Heldin, Laia Caja edited the revised version of the manuscript. All authors critically edited and revised the article and approved its submission for publication.

ACKNOWLEDGMENTS

We thank members of our laboratory for discussions, Masato Morikawa for reagents and Maria Tsioumpekou for technical advice. Confocal analysis was performed at the BioVis facility of Uppsala University with the kind involvement of Dirk Pacholsky. This work was supported by the Ludwig Cancer Research (Uppsala Branch); Cancerfonden [CAN 2015/438, CAN 2018/469] to A. M.; Barncancerfonden [PR2020-0088] to A. M., [TJ2021-0078] to Y. O.; Vetenskapsrådet [2017-01588-3, 2018-02757-3] to A. M., [2015-02757, 2020-01291] to C.-H. H.; the European Research Council [787472] to C.-H. H.; OE och Edla Johanssons Stiftelse [2018, 2019], Petrus och Augusta Hedlunds Stiftelse [M2019-1065, M2020-1274], Svenska Läkaresällskapet's Fonder [SLS-887701], Magnus Bergvalls

FIGURE 8 *SNAI1* silencing partially rescues the defective acinar morphogenesis of *LKB1* knockout cells. (a) Cumulative qRT-PCR analysis of *SNAI1* expression in parental MCF10A and *LKB1* knockout cells after silencing of endogenous *SNAI1* and treatment, or not (Cntl), with 5 ng/ml TGF β 1 for 24 or 48 h. Data are presented as mean values of three technical replicates \pm SEM, each in technical triplicates with *p* values calculated based on a two-tailed unpaired Student's *t*-test. (b) Representative immunoblot of *SNAI1*, p-SMAD2, PAI-1, fibronectin, and LKB1, in parental MCF10A and *LKB1* knockout cells after silencing of endogenous *SNAI1* in the absence or presence of 5 ng/ml TGF β for 2 or 24 h. β -Actin served as loading control. Molecular size markers in kDa are shown and original immunoblots are shown in Supporting Information: Figure S10. (c) Representative phase-contrast images of 12-day parental MCF10A and *LKB1* knockout acini cultured in matrigel that were either untreated or treated with 5 ng/ml TGF β 1 after transfection with control or *SNAI1*-specific siRNAs. Scale bar, 20 μ m. (d) Quantification of intact and protruding acini from the experiment of panel c, presented as bar graph measuring the percent of intact mammospheres and of mammospheres exhibiting protrusions into the surrounding matrigel. The data are derived from the analysis of 417 mammospheres in total (*n* = 80, 69, 92, 66, 65, 45, conditions No. 1-6, respectively). Representative of *n* = 2 independent biological experiments. (e) Quantification of parental MCF10A cell organoid size (spherical diameter in μ m) after silencing of endogenous *SNAI1* and treatment with 5 ng/ml TGF β 1 for 4 days. The data are presented as box and whisker plots of the triplicates with median values (\times), minimum and maximum values (whiskers), upper and lower quartile values (boxes), and *p* values shown based on a two-tailed unpaired Student's *t*-test. *p* Values. LKB1, liver kinase B1; qRT-PCR, quantitative Real-Time polymerase chain reaction; SEM, standard errors of the mean; TGF β , transforming growth factor β .

Stiftelse [2019-03444, 2020-03781] and Lars Hiertas Stiftelse [FO2020-0335] to L. C.

CONFLICT OF INTEREST STATEMENT

The authors declare no conflict of interest.

ETHICS STATEMENT

All experimental procedures and use of clinical samples were approved by the ethics committee of the Faculty of Medicine, Tokyo Medical and Dental University (registration number M2000-1458). All studies were conducted in accordance with the ethical guidelines of the amendment of the Declaration of Helsinki. All authors have provided written consent for publication.

ORCID

Laia Caja  <http://orcid.org/0000-0002-8786-8763>

Aristidis Moustakas  <http://orcid.org/0000-0001-9131-3827>

REFERENCES

- Alessi, D. R., Sakamoto, K., & Bayascas, J. R. (2006). LKB1-dependent signaling pathways. *Annual Review of Biochemistry*, 75, 137–163. <https://doi.org/10.1146/annurev.biochem.75.103004.142702>
- Baas, A. F., Kuipers, J., van der Wel, N. N., Battle, E., Koerten, H. K., Peters, P. J., & Clevers, H. C. (2004). Complete polarization of single intestinal epithelial cells upon activation of LKB1 by STRAD. *Cell*, 116(3), 457–466. [https://doi.org/10.1016/s0092-8674\(04\)00114-x](https://doi.org/10.1016/s0092-8674(04)00114-x)
- Budi, E. H., Muthusamy, B. P., & Derynck, R. (2015). The insulin response integrates increased TGF- β signaling through Akt-induced enhancement of cell surface delivery of TGF- β receptors. *Science Signaling*, 8(396), ra96. <https://doi.org/10.1126/scisignal.aaa9432>
- Chen, I. C., Chang, Y. C., Lu, Y. S., Chung, K. P., Huang, C. S., Lu, T. P., Kuo, W. H., Wang, M. Y., Kuo, K. T., Wu, P. F., Hsueh, T. H., Shen, C. Y., Lin, C. H., & Cheng, A. L. (2016). Clinical relevance of liver kinase B1(LKB1) protein and gene expression in breast cancer. *Scientific Reports*, 6, 21374. <https://doi.org/10.1038/srep21374>
- Cruz, V. H., & Brekken, R. A. (2018). Assessment of TANK-binding kinase 1 as a therapeutic target in cancer. *Journal of Cell Communication and Signaling*, 12(1), 83–90. <https://doi.org/10.1007/s12079-017-0438-y>
- Debnath, J., Muthusamy, S. K., & Brugge, J. S. (2003). Morphogenesis and oncogenesis of MCF-10A mammary epithelial acini grown in three-dimensional basement membrane cultures. *Methods*, 30(3), 256–268. [https://doi.org/10.1016/s1046-2023\(03\)00032-x](https://doi.org/10.1016/s1046-2023(03)00032-x)
- Deng, T., Liu, J. C., Chung, P. E. D., Uehling, D., Aman, A., Joseph, B., Ketela, T., Jiang, Z., Schachter, N. F., Rottapel, R., Egan, S. E., Al-awar, R., Moffat, J., & Zacksenhaus, E. (2014). shRNA kinome screen identifies TBK1 as a therapeutic target for HER2⁺ breast cancer. *Cancer Research*, 74(7), 2119–2130. <https://doi.org/10.1158/0008-5472.CAN-13-2138>
- Fogg, V. C., Liu, C. J., & Margolis, B. (2005). Multiple regions of Crumbs3 are required for tight junction formation in MCF10A cells. *Journal of Cell Science*, 118, (Pt 13) 2859–2869. <https://doi.org/10.1242/jcs.02412>
- Fu, D., Wakabayashi, Y., Ido, Y., Lippincott-Schwartz, J., & Arias, I. M. (2010). Regulation of bile canalicular network formation and maintenance by AMP-activated protein kinase and LKB1. *Journal of Cell Science*, 123, (Pt 19) 3294–3302. <https://doi.org/10.1242/jcs.068098>
- Goodwin, J. M., Svensson, R. U., Lou, H. J., Winslow, M. M., Turk, B. E., & Shaw, R. J. (2014). An AMPK-independent signaling pathway downstream of the LKB1 tumor suppressor controls Snail1 and metastatic potential. *Molecular Cell*, 55(3), 436–450. <https://doi.org/10.1016/j.molcel.2014.06.021>
- Hao, J., Ho, J. N., Lewis, J. A., Karim, K. A., Daniels, R. N., Gentry, P. R., Hopkins, C. R., Lindsley, C. W., & Hong, C. C. (2010). In vivo structure-activity relationship study of dorsomorphin analogues identifies selective VEGF and BMP inhibitors. *ACS Chemical Biology*, 5(2), 245–253. <https://doi.org/10.1021/cb9002865>
- Hollstein, P. E., Eichner, L. J., Brun, S. N., Kamireddy, A., Svensson, R. U., Vera, L. I., Ross, D. S., Rymoff, T. J., Hutchins, A., Galvez, H. M., Williams, A. E., Shokhirev, M. N., Sreaton, R. A., Berdeaux, R., & Shaw, R. J. (2019). The AMPK-related kinases SIK1 and SIK3 mediate key tumor-suppressive effects of LKB1 in NSCLC. *Cancer Discovery*, 9(11), 1606–1627. <https://doi.org/10.1158/2159-8290.CD-18-1261>
- Hong, B., Zhang, J., & Yang, W. (2017). Activation of the LKB1-SIK1 signaling pathway inhibits the TGF- β -mediated epithelial-mesenchymal transition and apoptosis resistance of ovarian carcinoma cells. *Molecular Medicine Reports*, 17(2), 2837–2844. <https://doi.org/10.3892/mmr.2017.8229>
- Jensen, T. E., Rose, A. J., Jørgensen, S. B., Brandt, N., Schjerling, P., Wojtaszewski, J. F. P., & Richter, E. A. (2007). Possible CaMKK-dependent regulation of AMPK phosphorylation and glucose uptake at the onset of mild tetanic skeletal muscle contraction. *American Journal of Physiology-Endocrinology and Metabolism*, 292(5), E1308–E1317. <https://doi.org/10.1152/ajpendo.00456.2006>
- Kahata, K., Dadras, M. S., & Moustakas, A. (2018). TGF- β family signaling in epithelial differentiation and Epithelial-Mesenchymal transition. *Cold Spring Harbor Perspectives in Biology*, 10(1), a022194. <https://doi.org/10.1101/cshperspect.a022194>
- Kahata, K., Maturi, V., & Moustakas, A. (2018). TGF- β family signaling in ductal differentiation and branching morphogenesis. *Cold Spring Harbor Perspectives in Biology*, 10(3), a031997. <https://doi.org/10.1101/cshperspect.a031997>
- Lahn, M., Hertzberg, S., Sawyer, J. S., Stauber, A. J., Gueorgieva, I., Driscoll, K. E., Estrem, S. T., Cleverly, A. L., Desai, D., Guba, S. C., Benhadji, K. A., & Slapak, C. A. (2015). Clinical development of galunisertib (LY2157299 monohydrate), a small molecule inhibitor of transforming growth factor-beta signaling pathway. *Drug Design, Development and Therapy*, 9, 4479–4499. <https://doi.org/10.2147/DDDT.S86621>
- Lambert, A. W., & Weinberg, R. A. (2021). Linking EMT programmes to normal and neoplastic epithelial stem cells. *Nature Reviews Cancer*, 21(5), 325–338. <https://doi.org/10.1038/s41568-021-00332-6>
- Li, J., Liu, J., Li, P., Mao, X., Li, W., Yang, J., & Liu, P. (2014). Loss of LKB1 disrupts breast epithelial cell polarity and promotes breast cancer metastasis and invasion. *Journal of Experimental & Clinical Cancer Research*, 33, 70. <https://doi.org/10.1186/s13046-014-0070-0>
- Li, N. S., Zou, J. R., Lin, H., Ke, R., He, X. L., Xiao, L., Huang, D., Luo, L., Lv, N., & Luo, Z. (2016). LKB1/AMPK inhibits TGF- β 1 production and the TGF- β signaling pathway in breast cancer cells. *Tumor Biology*, 37(6), 8249–8258. <https://doi.org/10.1007/s13277-015-4639-9>
- Lin, H., Li, N., He, H., Ying, Y., Sunkara, S., Luo, L., Lv, N., Huang, D., & Luo, Z. (2015). AMPK inhibits the stimulatory effects of TGF- β on Smad2/3 activity, cell migration, and Epithelial-to-Mesenchymal transition. *Molecular Pharmacology*, 88(6), 1062–1071. <https://doi.org/10.1124/mol.115.099549>
- Marignani, P. A., Kanai, F., & Carpenter, C. L. (2001). LKB1 associates with Brg1 and is necessary for Brg1-induced growth arrest. *Journal of Biological Chemistry*, 276(35), 32415–32418. <https://doi.org/10.1074/jbc.C100207200>
- Martin, S. G., & St Johnston, D. (2003). A role for *Drosophila* LKB1 in anterior-posterior axis formation and epithelial polarity. *Nature*, 421(6921), 379–384. <https://doi.org/10.1038/nature01296>

- Mehenni, H., Gehrig, C., Nezu, J., Oku, A., Shimane, M., Rossier, C., Guex, N., Blouin, J. L., Scott, H. S., & Antonarakis, S. E. (1998). Loss of LKB1 kinase activity in Peutz-Jeghers syndrome, and evidence for allelic and locus heterogeneity. *The American Journal of Human Genetics*, 63(6), 1641–1650. <https://doi.org/10.1086/302159>
- Merlin, J., Evans, B. A., Csikasz, R. I., Bengtsson, T., Summers, R. J., & Hutchinson, D. S. (2010). The M3-muscarinic acetylcholine receptor stimulates glucose uptake in L6 skeletal muscle cells by a CaMKK-AMPK-dependent mechanism. *Cellular Signalling*, 22(7), 1104–1113. <https://doi.org/10.1016/j.cellsig.2010.03.004>
- Morén, A., Raja, E., Heldin, C.-H., & Moustakas, A. (2011). Negative regulation of TGF β signaling by the kinase LKB1 and the scaffolding protein LIP1. *Journal of Biological Chemistry*, 286(1), 341–353. <https://doi.org/10.1074/jbc.M110.190660>
- Moustakas, A., & Heldin, C.-H. (2012). Induction of epithelial-mesenchymal transition by transforming growth factor β . *Seminars in Cancer Biology*, 22(5–6), 446–454. <https://doi.org/10.1016/j.semcancer.2012.04.002>
- Murray, C. W., Brady, J. J., Tsai, M. K., Li, C., Winters, I. P., Tang, R., Andrejka, L., Ma, R. K., Kunder, C. A., Chu, P., & Winslow, M. M. (2019). An LKB1-SIK axis suppresses lung tumor growth and controls differentiation. *Cancer Discovery*, 9(11), 1590–1605. <https://doi.org/10.1158/2159-8290.CD-18-1237>
- Muthuswamy, S. K., Li, D., Lelievre, S., Bissell, M. J., & Brugge, J. S. (2001). ErbB2, but not ErbB1, reinitiates proliferation and induces luminal repopulation in epithelial acini. *Nature Cell Biology*, 3(9), 785–792. <https://doi.org/10.1038/ncb0901-785>
- Nezu, J., Oku, A., & Shimane, M. (1999). Loss of cytoplasmic retention ability of mutant LKB1 found in Peutz-Jeghers syndrome patients. *Biochemical and Biophysical Research Communications*, 261(3), 750–755. <https://doi.org/10.1006/bbrc.1999.1047>
- Partanen, J. I., Nieminen, A. I., Mäkelä, T. P., & Klefstrom, J. (2007). Suppression of oncogenic properties of c-Myc by LKB1-controlled epithelial organization. *Proceedings of the National Academy of Sciences*, 104(37), 14694–14699. <https://doi.org/10.1073/pnas.0704677104>
- Partanen, J. I., Tervonen, T. A., & Klefström, J. (2013). Breaking the epithelial polarity barrier in cancer: the strange case of LKB1/Par-4. *Philosophical Transactions of the Royal Society, B: Biological Sciences*, 368(1629), 20130111. <https://doi.org/10.1098/rstb.2013.0111>
- Partanen, J. I., Tervonen, T. A., Myllynen, M., Lind, E., Imai, M., Katajisto, P., Dijkgraaf, G. J. P., Kovanen, P. E., Mäkelä, T. P., Werb, Z., & Klefström, J. (2012). Tumor suppressor function of liver kinase B1 (Lkb1) is linked to regulation of epithelial integrity. *Proceedings of the National Academy of Sciences*, 109(7), E388–E397. <https://doi.org/10.1073/pnas.1120421109>
- Raja, E., Tzavlaki, K., Vuilleumier, R., Edlund, K., Kahata, K., Zieba, A., Morén, A., Watanabe, Y., Voytyuk, I., Botling, J., Söderberg, O., Micke, P., Pyrowolakis, G., Heldin, C. H., & Moustakas, A. (2016). The protein kinase LKB1 negatively regulates bone morphogenetic protein receptor signaling. *Oncotarget*, 7(2), 1120–1143. <https://doi.org/10.18632/oncotarget.6683>
- Reginato, M. J., Mills, K. R., Becker, E. B. E., Lynch, D. K., Bonni, A., Muthuswamy, S. K., & Brugge, J. S. (2005). Bim regulation of lumen formation in cultured mammary epithelial acini is targeted by oncogenes. *Molecular and Cellular Biology*, 25(11), 4591–4601. <https://doi.org/10.1128/MCB.25.11.4591-4601.2005>
- Rhodes, L. V., Tate, C. R., Hoang, V. T., Burks, H. E., Gilliam, D., Martin, E. C., Elliott, S., Miller, D. B., Buechlein, A., Rusch, D., Tang, H., Nephew, K. P., Burow, M. E., & Collins-Burow, B. M. (2015). Regulation of triple-negative breast cancer cell metastasis by the tumor-suppressor liver kinase B1. *Oncogenesis*, 4, e168. <https://doi.org/10.1038/oncsis.2015.27>
- Rodríguez-Fraticelli, A. E., Auzan, M., Alonso, M. A., Bornens, M., & Martín-Belmonte, F. (2012). Cell confinement controls centrosome positioning and lumen initiation during epithelial morphogenesis. *Journal of Cell Biology*, 198(6), 1011–1023. <https://doi.org/10.1083/jcb.201203075>
- Sebbagh, M., Santoni, M. J., Hall, B., Borg, J. P., & Schwartz, M. A. (2009). Regulation of LKB1/STRAD localization and function by E-cadherin. *Current Biology*, 19(1), 37–42. <https://doi.org/10.1016/j.cub.2008.11.033>
- Seton-Rogers, S. E., Lu, Y., Hines, L. M., Koundinya, M., LaBaer, J., Muthuswamy, S. K., & Brugge, J. S. (2004). Cooperation of the ErbB2 receptor and transforming growth factor β in induction of migration and invasion in mammary epithelial cells. *Proceedings of the National Academy of Sciences*, 101(5), 1257–1262. <https://doi.org/10.1073/pnas.0308090100>
- Shackelford, D. B., & Shaw, R. J. (2009). The LKB1-AMPK pathway: metabolism and growth control in tumour suppression. *Nature Reviews Cancer*, 9(8), 563–575. <https://doi.org/10.1038/nrc2676>
- Shaw, R. J., Kosmatka, M., Bardeesy, N., Hurley, R. L., Witters, L. A., DePinho, R. A., & Cantley, L. C. (2004). The tumor suppressor LKB1 kinase directly activates AMP-activated kinase and regulates apoptosis in response to energy stress. *Proceedings of the National Academy of Sciences*, 101(10), 3329–3335. <https://doi.org/10.1073/pnas.0308061100>
- Sun, Y., Connors, K. E., & Yang, D. Q. (2007). AICAR induces phosphorylation of AMPK in an ATM-dependent, LKB1-independent manner. *Molecular and Cellular Biochemistry*, 306(1–2), 239–245. <https://doi.org/10.1007/s11010-007-9575-6>
- Sundqvist, A., Vasilaki, E., Voytyuk, O., Bai, Y., Morikawa, M., Moustakas, A., Miyazono, K., Heldin, C. H., ten Dijke, P., & van Dam, H. (2020). TGF β and EGF signaling orchestrates the AP-1- and p63 transcriptional regulation of breast cancer invasiveness. *Oncogene*, 39(22), 4436–4449. <https://doi.org/10.1038/s41388-020-1299-z>
- Syed, B. M., Green, A. R., Morgan, D. A. L., Ellis, I. O., & Cheung, K. L. (2019). Liver kinase B1-A potential therapeutic target in Hormone-Sensitive breast cancer in older women. *Cancers*, 11(2), 149. <https://doi.org/10.3390/cancers11020149>
- Takeda, S., Iwai, A., Nakashima, M., Fujikura, D., Chiba, S., Li, H. M., Uehara, J., Kawaguchi, S., Kaya, M., Nagoya, S., Wada, T., Yuan, J., Rayter, S., Ashworth, A., Reed, J. C., Yamashita, T., Ueda, T., & Miyazaki, T. (2007). LKB1 is crucial for TRAIL-mediated apoptosis induction in osteosarcoma. *Anticancer Research*, 27(2), 761–768.
- Tiainen, M. (2002). Growth arrest by the LKB1 tumor suppressor: induction of p21^{WAF1/CIP1}. *Human Molecular Genetics*, 11(13), 1497–1504. <https://doi.org/10.1093/hmg/11.13.1497>
- Tsubakihara, Y., & Moustakas, A. (2018). Epithelial-Mesenchymal transition and metastasis under the control of transforming growth factor β . *International Journal of Molecular Sciences*, 19(11), 3672. <https://doi.org/10.3390/ijms19113672>
- Vidi, P. A., Bissell, M. J., & Lelièvre, S. A. (2013). Three-dimensional culture of human breast epithelial cells: the how and the why. *Methods in Molecular Biology*, 945, 193–219. https://doi.org/10.1007/978-1-62703-125-7_13
- Wang, H., Lacoche, S., Huang, L., Xue, B., & Muthuswamy, S. K. (2013). Rotational motion during three-dimensional morphogenesis of mammary epithelial acini relates to laminin matrix assembly. *Proceedings of the National Academy of Sciences*, 110(1), 163–168. <https://doi.org/10.1073/pnas.1201141110>
- Watts, J. L., Morton, D. G., Bestman, J., & Kempthues, K. J. (2000). The *C. elegans par-4* gene encodes a putative serine-threonine kinase required for establishing embryonic asymmetry. *Development*, 127(7), 1467–1475.
- Williams, C. M., Engler, A. J., Slone, R. D., Galante, L. L., & Schwarzbauer, J. E. (2008). Fibronectin expression modulates mammary epithelial cell proliferation during acinar differentiation.

Cancer Research, 68(9), 3185–3192. <https://doi.org/10.1158/0008-5472.CAN-07-2673>

- Woods, A., Johnstone, S. R., Dickerson, K., Leiper, F. C., Fryer, L. G. D., Neumann, D., Schlattner, U., Wallimann, T., Carlson, M., & Carling, D. (2003). LKB1 is the upstream kinase in the AMP-activated protein kinase cascade. *Current Biology*, 13(22), 2004–2008. <https://doi.org/10.1016/j.cub.2003.10.031>
- Xu, X., Jin, D., Durgan, J., & Hall, A. (2013). LKB1 controls human bronchial epithelial morphogenesis through p114RhoGEF-dependent RhoA activation. *Molecular and Cellular Biology*, 33(14), 2671–2682. <https://doi.org/10.1128/MCB.00154-13>
- Zeqiraj, E., Filippi, B. M., Deak, M., Alessi, D. R., & van Aalten, D. M. F. (2009). Structure of the LKB1-STRAD-MO25 complex reveals an allosteric mechanism of kinase activation. *Science*, 326(5960), 1707–1711. <https://doi.org/10.1126/science.1178377>
- Zhan, L., Rosenberg, A., Bergami, K. C., Yu, M., Xuan, Z., Jaffe, A. B., Allred, C., & Muthuswamy, S. K. (2008). Deregulation of scribble promotes mammary tumorigenesis and reveals a role for cell polarity in carcinoma. *Cell*, 135(5), 865–878. <https://doi.org/10.1016/j.cell.2008.09.045>
- Zhang, Y., Unnithan, R. V. M., Hamidi, A., Caja, L., Saupe, F., Moustakas, A., Cedervall, J., & Olsson, A. K. (2019). TANK-binding kinase 1 is a mediator of platelet-induced EMT in mammary carcinoma cells. *The*

FASEB Journal, 33(7), 7822–7832. <https://doi.org/10.1096/fj.201801936RRR>

SUPPORTING INFORMATION

Additional supporting information can be found online in the Supporting Information section at the end of this article.

How to cite this article: Tzavlaki, K., Ohata, Y., Morén, A., Watanabe, Y., Eriksson, J., Tsuchiya, M., Kubo, Y., Yamamoto, K., Sellin, M. E., Kato, M., Caja, L., Heldin, C.-H., & Moustakas, A. (2023). The liver kinase B1 supports mammary epithelial morphogenesis by inhibiting critical factors that mediate epithelial-mesenchymal transition. *Journal of Cellular Physiology*, 238, 790–812. <https://doi.org/10.1002/jcp.30975>